Universidade de Aveiro Departamento de Biologia
Ano 2017

Joana Filipa Marques Santiago

Modulação da mobilidade dos espermatozoides recorrendo a *cell-penetrating peptides*

Modulation of sperm motility using cell-penetrating peptides

DECLARAÇÃO

Declaro que este relatório é integralmente da minha autoria, estando devidamente referenciadas as fontes e obras consultadas, bem como identificadas de modo claro as citações dessas obras. Não contém, por isso, qualquer tipo de plágio quer de textos publicados, qualquer que seja o meio dessa publicação, incluindo meios eletrónicos, quer de trabalhos académicos.

Universidade de Aveiro Departamento de Biologia
Ano 2017

Joana Filipa Marques Santiago

Modulação da mobilidade de espermatozoides recorrendo a *cell-penetrating peptides*

Modulation of sperm motility using cell-penetrating peptides

Dissertação apresentada à Universidade de Aveiro para cumprimento dos requisitos necessários à obtenção do grau de Mestre em Biologia Molecular e Celular, realizada sob a orientação científica da Doutora Margarida Sâncio da Cruz Fardilha, Professora Auxiliar do Departamento de Ciências Médicas da Universidade de Aveiro e coorientação da Doutora Joana Vieira Silva, Investigadora de Pós-Doutoramento do Instituto de Biomedicina da Universidade de Aveiro, e da Doutora Maria de Lourdes Gomes Pereira, Professora Associada com Agregação do Departamento de Biologia da Universidade de Aveiro.

Este trabalho é financiado por Fundos FEDER através do Programa Operacional Fatores de Competitividade -COMPETE e por Fundos Nacionais através da FCT – Fundação para a Ciência e a Tecnologia no âmbito do projeto «PTDC/BBB-BQB/3804/2014»; e do Instituto de Biomedicina -iBiMED «UID/BIM/04501/2013».

o júri

presidente

Prof. Doutora Maria Helena Abreu Silva
professor auxiliar do Departamento de Biologia da Universidade de Aveiro

Prof. Doutor Pedro Fontes Oliveira
professor afiliado do Instituto de Ciências Biomédicas Abel Salazar da Universidade do Porto

Doutora Joana Vieira Silva
Investigador de Pós-doutoramento do Instituto de Biomedicina da Universidade de Aveiro

agradecimentos

À minha orientadora, Doutora Margarida Fardilha, pela ajuda que me deu ao longo deste ano e pela oportunidade que me deu de integrar esta equipa fantástica e dinâmica. Muito obrigada pela disponibilidade e por todo o apoio.

À minha coorientadora, Doutora Joana Vieira Silva, por ter sido bem mais do que uma orientadora ao longo deste ano. Por todo o conhecimento que me transmitiu, por todo o apoio, tanto a nível profissional como pessoal, e por toda a confiança que depositou em mim e no meu trabalho. Obrigada pela forma carinhosa como me acolheste, é um privilégio trabalhar contigo.

À Professora Maria de Lourdes Pereira, por todo o apoio e pela disponibilidade.

A todos os meus colegas no Laboratório de Transdução de Sinal. Em especial à Daniela, Juliana, Magda, Maria e Sofia, que se tornaram mais do que colegas de trabalho. Obrigada por me integrarem no vosso grupo de trabalho e por todo o apoio. Obrigada por me mostrarem que o trabalho pode ser divertido.

Ao Joel, por estar sempre do meu lado.

A toda a minha família, por estarem sempre presentes. Em especial aos meus pais, pelo incansável apoio e carinho e por tornarem tudo isto possível. Obrigada por tudo.

À minha irmã, por mesmo longe estar sempre perto.

palavras-chave

espermatozoides, mobilidade, *cell-penetrating peptides*, fosfoproteína fosfatase 1, interação proteína-proteína, complexos proteicos

resumo

O elevado número de gravidezes indesejadas a nível mundial e o facto de os contracetivos masculinos estarem limitados ao preservativo e à vasectomia refletem a necessidade urgente de desenvolvimento de novos métodos contracetivos. O mecanismo de aquisição de mobilidade dos espermatozoides no epidídimo constitui um alvo perfeito para novos agentes contracetivos dado que apenas a maturação pós-testicular é afetada. Sabe-se que a proteína fosfatase 1 subunidade gama 2 (PPP1CC2), uma isoforma presente apenas nos testículos e espermatozoides, é essencial para a aquisição de mobilidade no epidídimo. As interações proteína-proteína (PPIs) têm surgido como uma promissora classe de alvos terapêuticos e os *cell-penetrating peptides* (CPPs) representam um reconhecido sistema de entrega intracelular de sequências peptídicas com o potencial de modular PPIs. Assim, o principal objetivo deste trabalho é modular complexos PPP1CC2 específicos de testículo e espermatozoide e, consequentemente, a mobilidade dos espermatozoides recorrendo a sequências peptídicas covalentemente ligadas a CPPs. Os resultados mostram que ambos os péptidos testados são capazes de modular a mobilidade dos espermatozoides, mesmo com curtos períodos de incubação, aumentando o número de espermatozoides imóveis. Adicionalmente, foi demonstrado que o péptido que mimetiza a interface de interação entre PPP1CC2 e uma a A-kinase anchor protein (AKAP4) – um interactor específico no espermatozoide – interfere com a interação PPP1CC2-AKAP4, resultando em espermatozoides imóveis. O péptido que mimetiza os 22 aminoácidos do C-terminal da PPP1CC2 atua disrompendo a interação entre a PPP1CC2 e interatores específicos desta isoforma. Cinquenta interatores específicos do C-terminal da PPP1CC2 foram identificados por espectrometria de massa, sugerindo novos potenciais alvos para futura modulação. Um desses interatores (GPx4) foi posteriormente validado.

Concluindo, este trabalho confirmou o potencial dos CPPs na entrega de sequências peptídicas que têm como alvo PPIs únicas do espermatozoide, clarificou o mecanismo de ação dos péptidos testados e identificou potenciais alvos para novos contracetivos masculinos.

keywords

spermatozoa, motility, cell-penetrating peptides, phosphoprotein phosphatase 1, protein-protein interaction, protein complexes

abstract

The large number of unintended pregnancies worldwide due to the non-use or failure of contraceptive methods and the fact that male contraceptives are limited to condom and vasectomy, highlight the urgent need for the development of new contraceptive methods. The mechanism of sperm motility acquisition in the epididymis constitutes an ideal target for new pharmacological male contraceptives since only the post-testicular sperm maturation is affected. It is known that protein phosphatase 1 subunit gamma 2 (PPP1CC2), a PPP1 isoform only present in testes and sperm, is essential for sperm motility acquisition. Protein-protein interactions (PPIs) have emerged as a promising class of drug targets and cell-penetrating peptides (CPPs) represents a recognized intracellular delivery system to target PPIs. The main goal of this work is to modulate PPP1CC2 complexes and, consequently, spermatozoa motility using peptides covalently coupled to CPPs. The results showed that both peptides tested could modulate sperm motility with a short incubation period, generally increasing the number of immotile spermatozoa. Additionally, we demonstrated that the peptide sequence that mimics the interaction interface between PPP1CC2 and a sperm-specific interactor – A-kinase anchor protein 4 (AKAP4) – disrupted the PPP1CC2-AKAP4 interaction, resulting in arrest of sperm motility. The peptide that mimics the 22 amino-acid C-terminus of PPP1CC2 possible acts by disrupting the interaction between PPP1CC2 and isoform-specific interactors. Fifty putative isoform-specific interactors of PPP1CC2 C-terminus were identified by mass spectrometry and one of them was further validated (GPx4), suggesting new targets for similar contraceptive agents.

In conclusion, this work confirmed the potential of CPPs to deliver peptide sequences that target unique PPIs in spermatozoa, clarified the mechanism of action of the peptides testes and identified other potential targets for new male contraceptives.

Table of Contents

List of Figures

List of Tables

List of Abbreviations, symbols and acronyms

AKAP	A-kinase anchor protein
AKAP4-BM	A-kinase anchor protein binding motif
AKAP4-BM M	Mutated A-kinase anchor protein binding motif
APS	Ammonium persulfate
ATP	Adenosine triphosphate
BCA	Bicinchoninic acid
BSA	Bovine serum albumin
cAMP	Cyclic adenosine monophosphate
CASA	Computer aided sperm analyser
CDK	Cyclin-dependent kinase
cDNA	Complementary deoxyribonucleic acid
CO-IP	Co-immunoprecipitation
CP	Central pair
CPP	Cell-penetrating peptide
DA	Dynein arms
DMEM	Dulbecco's Modified Eagle's Medium
DNA	Deoxyribonucleic acid
ERC	Excess of residual cytoplasm
FBS	Fetal bovine serum
FDR	False discovery rate
FS	Fibrous sheath
G3PD	Glyceraldehyde 3-phosphate dehydrogenase
GFP	Green fluorescent protein
GPx4	Glutathione peroxidase 4
GSK3	Glycogen-synthase kinase 3
HP	Homing peptide
HPA	Human protein atlas
IB	Immunoblot
IBiMED	Institute for Biomedicine
IM	Immotile
IP	Immunoprecipitation
LB	Loading buffer
LC-MS/MS	Liquid chromatography mass spectrometry

LFQ	Label-free quantitative analysis
LRP6	LDL receptor related protein 6
MP	Midpiece
mRNA	Messenger ribonucleic acid
MS	Mitochondrial sheath
NC	Negative control
NPM	Non-progressive motility
ODF	Outer dense fibres
OMDA	Outer microtubule doublets
PAGE	Polyacrylamide gel electrophoresis
PBS	Phosphate buffered saline
PDE4A	Phosphodiesterase 4A cAMP specific
PGK2	Phosphoglycerate kinase 2
PIP	PPP1 interacting protein
PKA	Protein kinase A
PM	Plasma membrane
PM	Progressive motility
PPI	Protein-protein interaction
PPP1	Phosphoprotein phosphatase 1
PPP1C	Phosphoprotein phosphatase 1 catalytic subunit
PPP1CC1	Phosphoprotein phosphatase 1 subunit gamma 1
PPP1CC2	Phosphoprotein phosphatase 1 subunit gamma 2
PPP1CC2-CT	Phosphoprotein phosphatase 1 subunit gamma 2 C-terminus
PPP1R11	Phosphoprotein phosphatase 1 inhibitor 3
PPP1R2	Phosphoprotein phosphatase 1 inhibitor 2
PPP1R3P3	Phosphoprotein phosphatase 1 inhibitor 2 pseudogene 3
PPP2CA	Phosphoprotein phosphatase 2 subunit alpha
PTM	Post-translation modifications
RNE	Redundant nuclear envelopes
RS	Radial spokes
RT	Room temperature
SCA	Sperm class analyser
SDS	Sodium dodecyl sulphate
SPZ1	Spermatogenic zip protein
TBS	Tris-buffered saline

TBST	Tris-buffered saline containing 0,1% Tween-20
Tctex5	t-complex expressed protein 5
TR	Transverse ribs
WHO	World Health Organization
WR	Working reagent

1. General Introduction and Aims

1.1. Spermatogenesis

Spermatogenesis is a highly regulated process that takes place within the seminiferous tubules and consists in the development of a diploid spermatogonium into a highly specialized haploid male gamete [1]. This process includes mitotic and meiotic divisions as well as extensive morphological alterations [2], and can be divided in four steps: (i) self-renewal and differentiation of spermatogonia, (ii) meiosis, (iii) spermiogenesis and (iv) spermiation [3,4]. The first phase consists in self-renewal of A dark and A pale spermatogonia and differentiation of A pale spermatogonia through mitosis producing type B spermatogonia [5]. Type B spermatogonia divide mitotically originating primary spermatocytes [2]. On phase ii, spermatocytogenesis, the primary spermatocyte undergoes two meiotic cycles giving rise to haploid spermatids [2]. Spermiogenesis consists in the differentiation of the spermatid into a spermatozoon and includes a complex sequence of events. The acrosome and flagellum are developed, chromatin condensation occurs and histones are changed by protamines, the excess of cytoplasm is removed, development of the tail and reorganization of cellular organelles such as centrioles and mitochondria takes place [2,4]. At this point the spermatid can be released to the tubule lumen, a process designated by spermiation. This process is highly regulated by complex signaling mechanisms involving the hypothalamic-pituitary-gonadal axis, leading to the continuous production of spermatozoa starting from puberty through the reproductive life span of the male [4,6] (reviewed by Rossitto et al. [7]).

In humans, spermatogenesis takes approximately 74 days [2] but Misell *et al*. (2006) have observed that the duration of spermatogenesis is very variable among individuals [8]. The duration of this process also varies between species, for example 35 days in the mouse and hamster, 41 days in wild boar [9], 40 day in pig and 47 to 48 in sheep [10].

1.2. Spermatozoa

The mammalian spermatozoa (Figure 1) consist of a head and a flagellum [11] and its length is specie-specific ranging between 50 μm (boar) to 90 μm (bull). In humans, it varies between 50 to 60 μm. Both head and flagellum are covered by plasma membrane [12].

1.2.1. Head

The sperm head comprises a nucleus and an acrosome surrounded by the plasma membrane [12]. The nucleus contains the condensed chromatin with the genetic information. The structure of chromatin changes dramatically during the final stages of spermiogenesis, when the DNA condensing core and linker histones are partially exchanged to protamines, positively charged DNA proteins that enable nuclear hyper condensation [13,14]. Despite the human sperm chromatin being tightly packaged by protamines, up to 4% of the DNA remains packaged by histones [15]. Infertile men have a higher sperm histone to protamine ratio when compared with fertile controls [16]. The nucleus is covered by a reduced nuclear envelope, from which the nuclear pore complexes have been removed during spermiogenesis, except for the redundant nuclear envelopes (RNEs) found in some species at the base of the sperm nucleus [17]. Sperm nucleus is protected by the perinuclear theca, forming a rigid shell composed of disulfide bond-stabilized structural proteins combined with various other proteins [18]. The acrosome is a Golgi-derived structure that covers two thirds of the anterior head surface [19]. The inner and outer membranes of the acrosome contain a dense acrosomal matrix that encloses a variety of proteases that are believed to digest a fertilization site in the zona pellucida. The equatorial segment (posterior acrosome) is a folded-over complex of perinuclear theca, inner and outer acrosomal membranes, which carries receptors involved in the sperm-egg fusion. [20].

1.2.2. Flagellum

The flagellum is the longest part of the sperm and is a critical structure for motility. The major cytoskeletal components of the flagellum are the axoneme, fibrous sheath (FS) and outer dense fibers (ODF). While the axoneme function as the motor of the sperm, the FS and ODF modulate the frequency and pattern of flagellar beating [21]. The axoneme extends the full length of the flagellum and is composed by nine microtubule doublet surrounding a central pair of microtubules called a “nine-plus-two” complex [12,21]. The peripheral pairs are partially fused and the microtubules of the central pair are separated. A protein called nexin is responsible for the link of one microtubule doublet to another and dynein is connected to peripheral pairs to generate propulsion force in the flagellum [22].
The flagellum is divided into connecting piece, mid-piece, principal piece and end piece [23,24]. The shortest part of the flagellum is the connecting piece that attach the head to the rest of flagellum [11,24]. The mid-piece is adjacent to the head and is characterized by the presence of a mitochondrial sheath (MS) that surrounds the axoneme and ODFs [12].

While the MS is restricted to the mid-piece, the ODFs extend into the principal piece of the flagellum [25]. The *annulus* (or Jensen's ring) marks the barrier between the mid-piece and principal piece and prevents a caudal displacement of the mitochondria during tail movement. The principal piece occupies nearly three-fourths of flagellum's length and is flanked anteriorly by the mid-piece and posteriorly by a short distal piece [11]. At the start of the principal piece, the MS terminates and two of the ODFs are replaced by two longitudinal columns of fibrous sheet (FS). The most abundant protein present in the FS is A-kinase anchor protein 4 (AKAP4), a PKA-anchoring testis-specific protein [21,26]. The FS columns define the length of the principal piece and are stabilized by circumferential ribs that surround the ODFs [23]. Usually all of the ODF are thickest in the proximal part of the middle piece and progressively diminish in diameter from the base to the tip of the tail [12]. The FS is the only structure that is restricted to the principal piece. The end piece is a short segment at the tip of the flagellum where the axoneme is only surrounded by a plasma membrane [12].

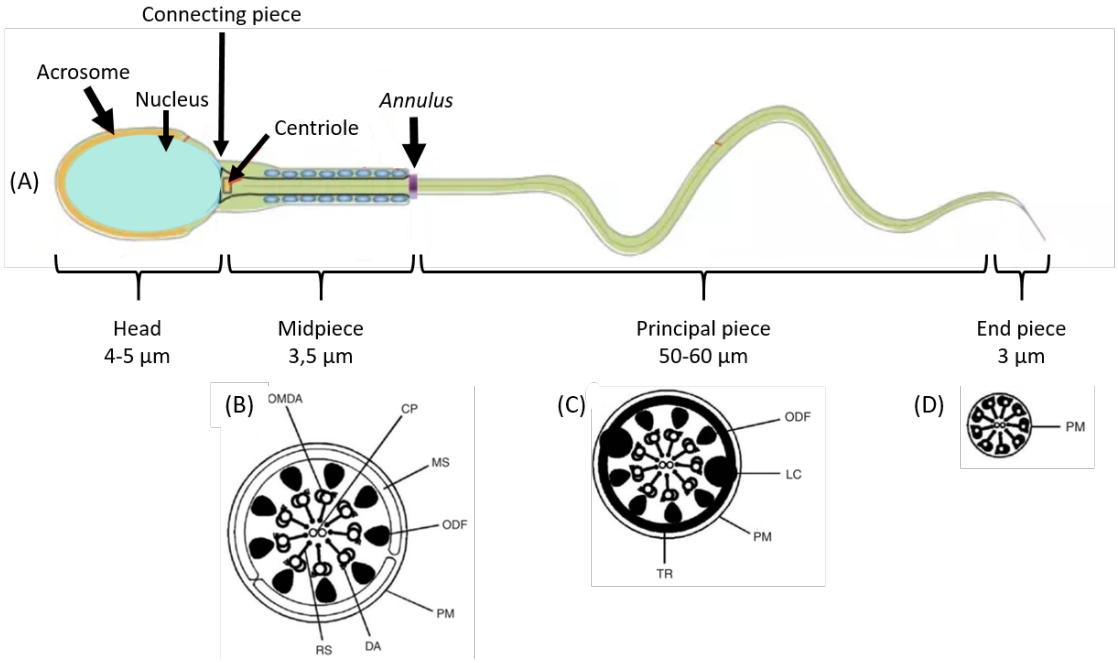

Figure 1 – Representation of the mammalian spermatozoa and the ultrastructure of the flagellum. (A) The flagellum is divided in four pieces: connection piece, middle piece, principal piece and end piece. The end of the middle piece and the start of the principal piece is demarcated by the annulus. (B) In a transversal cut through the middle piece is observed the plasma membrane (PM) and the mitochondrial sheath (MS) around nine outer dense fibers (ODF) and the axoneme. The axoneme is composed by nine outer microtubule doublets (OMDA) with associated dynein arms (DA) and radial spokes (RS) around a central pair of microtubules (CP). (C) Cross-section through the principal piece shows the PM surrounding seven ODF. The ODF 3 and 8 have been replaced by two longitudinal columns of fibrous sheath (FS) that are connected by transverse ribs (TR). (D)The final piece shows only plasma membrane and the axoneme. Adapted from [25].

1.3. Sperm Motility

The human sperm is a notable cell, characterized for its small size, lack of most organelles, almost devoided of transcription and translation, high polarity and fast motility [21]. Sperm motility can be defined as a propagation of transverse waves along the flagellum in a proximal-to-distal direction producing an impulse that pushes the spermatozoon through the female genital tract to reach and penetrate oocyte [27,28]. According with Paoli and colleagues, sperm motility results of many complexes processes like oxidation of energy substrates, phosphorylation of proteins involved in signal transduction cascades and conversion of chemical into mechanical energy in the axoneme [27]. The flagellar beat appears to be regulated by ATPase activity of axonemal dynein arms and modulated by alterations on pH, adenosine triphosphate (ATP) availability, calcium concentration and phosphorylation but the mechanism is not completely understood [25].

The motility is only acquired in the epididymis, where these cells become mature [28]. Spermatozoa motility patterns differ between the ejaculate and the fertilization site, and have been defined as activated and hyperactivated motility respectively. Immotile or poorly motile sperm is generally accepted like a clinical sign of infertility and the main cause is frequently unknown. In fact, very little is known about the mechanisms involved in regulating sperm motility so more research is crucial [29].

1.3.1. Epididymis and motility acquisition

When spermatozoa leave the testis, are morphological mature but functionally inactive so, incapable of fertilize the female gamete. Functionality is acquired during post-testicular maturation via mechanisms that are involved in acquisition, loss or post-translation modification of proteins [30]. The first step of maturation occurs in epididymis, a tightly coiled, highly differentiated structure present in all mammals that connects the efferent ducts of the testis to the vas deferens. It can be divided into anatomically distinct segments or regions: (i) caput (head), (ii) corpus (body), (iii) cauda (tail). In mammals, the epididymis has numerous functions including reabsorption of the fluid secreted by the seminiferous tubules and the maturation and storage of sperm [31]. Several studies showed that caput epididymal spermatozoa are immotile and do not show any progressive motility or flagella beating but spermatozoa obtained from caudal epididymis are highly motile [32]. During sperm maturation in the epididymis several biochemical and morphological changes occurs, resulting in progressive motility [33]. Those includes

changes in pH, intracellular concentrations of calcium ions and cyclic adenosine monophosphate (cAMP) that leads to shifts in protein phosphorylation status [30,34].

1.3.2. Activated and hyperactivated motility

There are two types of sperm motility patterns in most mammals: activated motility observed in the ejaculated spermatozoa and hyperactivated motility which is observed in spermatozoa at the site of fertilization [25,35,36] (Figure 2). Activated spermatozoa, show a symmetrical movement of flagellum and low-amplitude waveform that drives a sperm in a straight line in moderately non-viscous media such as seminal plasma [25,36]. This type of movement is acquired in epididymis and required in initial stages of sperm transport through the female reproductive tract [28]. This is regulated by phosphorylation mechanisms, being stimulated by phosphorylation in serine/threonine mechanisms [37]. When sperm reach the oviduct, the pattern of flagellar beat changes to an asymmetrical movement and higher amplitude, which results in a circular trajectory also known as a figure-8 trajectory [36,38]. This is called hyperactivated motility and is necessary to sperm progression in the oviduct, dissociation with the oviduct epithelium and to assist sperm in penetrating the cumulus oophorous and zona pellucida [28,39]. Although hyperactivation generally occurs at some point during capacitation, the pathways leading to capacitation and hyperactivation are not the same [40]. The initiation and maintenance of this type of motility patter *in vitro* requires several physiological factors such Ca^{2+}, bicarbonate and metabolic substrates [37,41].

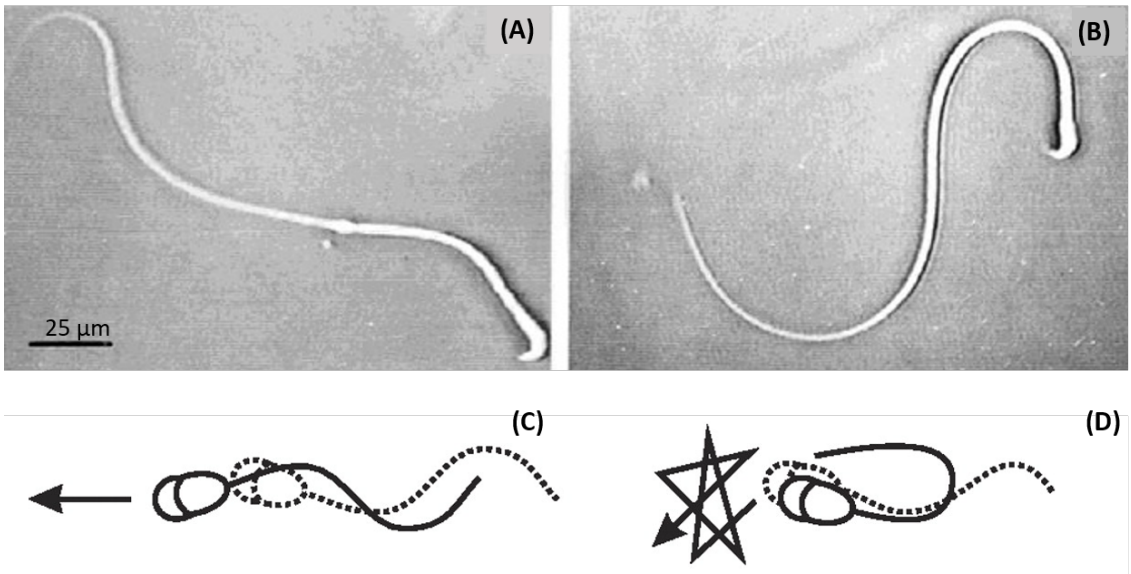

Figure 2 – Comparison of flagellar wave-forms of spermatozoa. Pictures of activated (A) and hyperactivated (B) hamster sperm from video records. Schematic representation of bending patterns of activated (C) and hyperactivated (D) morphological normal spermatozoa in low viscous medium. Adapted from [42].

1.3.3. Metabolic pathways to produce energy: oxidative phosphorylation and glycolysis

ATP is one of the key requirements for sperm motility, acting as a molecular motor for the flagellar movement [27]. In fact, ATP is the fuel used for axonemal dynein ATPases within the flagellum and is required in both activated and hyperactivated motility [35]. Also protein modification, such as phosphorylation, depends on ATP so it is not surprising that sperm requires more ATP than most type of cells [43]. Two metabolic pathways have been suggested for ATP production: mitochondrial respiration and glycolysis. Although the energy required for sperm motility be manly produced by oxidative phosphorylation in mitochondria at the middle piece, glycolysis seems to be an important source of ATP along the flagellum, occurring in the head and principal piece of the flagellum [35,44]. Mutations or environmental factors which compromise the activity of glycolytic enzymes, like glyceraldehyde 3-phosphate dehydrogenase (G3PD) or phosphoglycerate kinase 2 (PGK2), leads to a leak in energy production and then to immotile spermatozoa [45,46].

1.4. Role of Phosphoprotein Phosphatase 1 in sperm motility

1.4.1. Phosphoprotein Phosphatase 1 subunit gamma 2

Phosphoprotein phosphatase is a superfamily of proteins phosphatases which dephosphorylates serine and threonine residues [47]. This superfamily includes PPP1 to PPP7 differing only in their N- and C- terminus and sharing high homology in the catalytic domains [48–50]. PPP1 is responsible for about a third of all protein dephosphorylation reactions that occur in eukaryotic cells and the catalytic subunit (PPP1C) is encoded by three different genes (*PPP1CA*, *PPP1CB* and *PPP1CC)* being involved in the regulation of several cellular events like glycogen metabolism, cell cycle, and sperm motility [51]. After transcription, PPP1CC undergoes tissue-specific splicing, originating a ubiquitously expressed isoform, PPP1CC1, and a testis-enriched and sperm-specific isoform, PPP1CC2. The difference between these isoforms resides strictly in the C-terminal [51]. All four isoforms are expressed in mammalian testis [52,53] but PPP1CC2 is the isoform in higher amount in testis and spermatozoa [54]. PPP1CC2 is predominantly localized in post-meiotic cells, in the cytoplasm of secondary spermatocytes, round spermatids and elongated spermatids [52,53]. Some authors have showed that this phosphatase is involved in sperm tail morphogenesis. Varmuza *et al*. (1999) showed that the *Ppp1cc* gene deletion in mouse testis causes loss of both isoforms (PPP1CC1 and PPP1CC2) and results in male infertility due to impaired spermatogenesis. Disruption of *Ppp1cc*

result in malformed sperm tails, loss of mitochondrial sheaths and disorganized ODFs [55] as also showed by Chakrabarti and colleagues [52]. A recent study demonstrated that PPP1CC2, in the absence of PPP1CC1, restore sperm morphogenesis and sperm function in testis [56]. However, Soler and colleagues have observed that expression of transgenic PPP1CC2 in testis of *Ppp1cc*-null mice only restore spermatid viability and spermiation and not normal sperm tail morphology, motility or fertility [57].

1.4.2. PPP1CC2 and sperm motility acquisition in epididymis

Spermatozoa are specialized cells that are considered to be transcriptional inactive and incapable of synthetize new proteins so, protein phosphorylation is a post-translational mechanism that plays an important role in several events [58]. Protein phosphorylation is the net result of the action of protein kinases and phosphatases, and immotile sperm in the caput epididymis have significantly greater protein phosphatase activity than motile sperm in caudal epididymis [31].

PPP1CC2 is the only PPP1 isoform present along the entire flagellum including the mid-piece [59]. Since decreased PPP1CC2 activity is associated with increased motility, PPP1CC2 is thought to be a key protein for regulating sperm motility [52]. In fact, the inhibition of this protein activity in caudal sperm is connected to the onset of progressive motility and to a significant increase in vigorous movement in progressive motile sperm [33,60]. Okadaic acid and calyculin A are known PPP1 inhibitors and both initiate and stimulate motility in epididymal spermatozoa [33,60] and also promote hyperactivated sperm motility and acrosome reaction [42,61]. During epididymal sperm maturation the activity of PPP1 declines due to the lowering of its catalytic activity [62].

1.4.3. PPP1CC2 complexes in sperm motility

PPP1 exists in the cell as an oligomeric complex in which the PPP1C subunit binds to one or two regulatory subunits known as PPP1 Interacting Proteins (PIPs) that modulate its cellular localization, substrate specificity and activity [63,64]. More than 200 PIPs have been identified and they can be divided into PPP1C inhibitors, substrates, substrate-specifiers and targeting-subunits [63,65]. The binding of PIPs to PPP1C is mediated by short amino acid motifs and about 10 have already been described [66]. The best known PPP1 binding motif, is the RVxF, present in about 90% of all known PIPs and is thought to be the anchor for subsequent interactions [65]. The surface of PPP1 contains many binding sites for short PPP1-docking motifs that are combined by PIPs to create a PPP1-binding code [66] that is universal (PPP1C binding motifs are conserved along evolution),

specific (PPP1C binding motif does not bind to any related Phosphatase), degenerated (the amino acids in the binding motifs may have some flexibility which generates different binding affinities), nonexclusive (binding to a PIP does not exclude binding to a second PIP if the binding motif is different) and dynamic (there is molar excess of PIPs in comparison to PPP1C) [65]. Thus, depending on the PIP that is bound to PPP1C, the complex formed is involved in a specific cellular task [51].

PPP1CC2 activity during sperm maturation in the epididymis has been suggested to be mainly regulated by its inhibitors – PPP1R2 (inhibitor 2, I2), PPP1R7 (sds22) and PPP1R11 (inhibitor 3, I3) – by YWHA (14-3-3) and AKAPs [59] (Figure 3). Endophilin B1t, a testis enriched isoform of the somatic endophilin B1a, and the spermatogenic zip protein (Spz1) [67,68] are isoform-specific interactors. Both endophilin B1t and Spz1 do not interact with other PPP1C isoforms or with a truncated PPP1CC2 mutant lacking the unique C-terminus [67,68]. TMEM225, a protein predominantly localized to the equatorial segment in mature spermatozoa of mice, is also capable of bind to PPP1CC2 through RVxF motif and inhibit PPP1CC2. This evidence suggests that TMEM225 could regulate sperm motility and capacitation although its localization makes its contribution to motility less likely [69]. The role of these and other complexes in sperm motility still needs to be fully elucidated.

1.1.1.1 PPP1CC2/PPP1R2/GSK-3 Complex

PPP1R2 (I2) is a protein capable of inhibit the catalytic subunit of PPP1 leading to the production of a stable PPP1-PPP1R2 complex. Glycogen-synthase kinase (GSK)-3 is responsible for PPP1R2 phosphorylation at Thr73 resulting in the dissociation of PPP1 and PPP1R2 and, then, PPP1 becomes active [58,60,70]. In fact*, GSK3a* knockout mice is infertile due to impaired sperm motility but revealed high activity of PPP1CC2 in sperm [70]. Some studies have identified a PPP1R2-like activity and the presence of GSK-3 in mammalian sperm. Immotile bovine caput epididymal sperm contains 2-fold higher levels of protein phosphatase activity, identified as being PPP1CC2, and 6-fold higher GSK-3 activity than mature motile caudal sperm. Thus, the complex PPP1CC2/ PPP1R2-like is inactive in motile caudal sperm and the phosphatase activity is re-established in immotile sperm by the higher GSK-3 activity [33,60].

Korrodi-Gregório *et al.* have identified, by an yeast two-hybrid screen of a human testis library, a positive clone designated PPP1R2 pseudogene 3 (PPP1R3P3). PPP1R2P3 protein binds directly to PPP1CC and the inactive PPP1CC2-inhibitor complex formed cannot be activated by GSK-3 phosphorylation because there is no site for GSK-3 phosphorylation. PPP1R3P3 represents a constitutive inhibitor of PP1 that is independent

of GSK-3 phosphorylation [58]. One hypothesis might be that PPP1R3P3 is only present in caudal motile sperm, leading to constitutive inactivation of PP1CC2. Alternatively, PPP1R3P3 may be bound to a protein that keeps it from binding PP1CC2 in immotile caput sperm, paralleling what happens with PPP1R7 (sds22). The complex PP1CC2/PPP1R2/ GSK-3 may explain the unidirectional acquisition of sperm motility along the epididymal transit [59] and might be pre-requisites for the optimum function of spermatozoa [71].

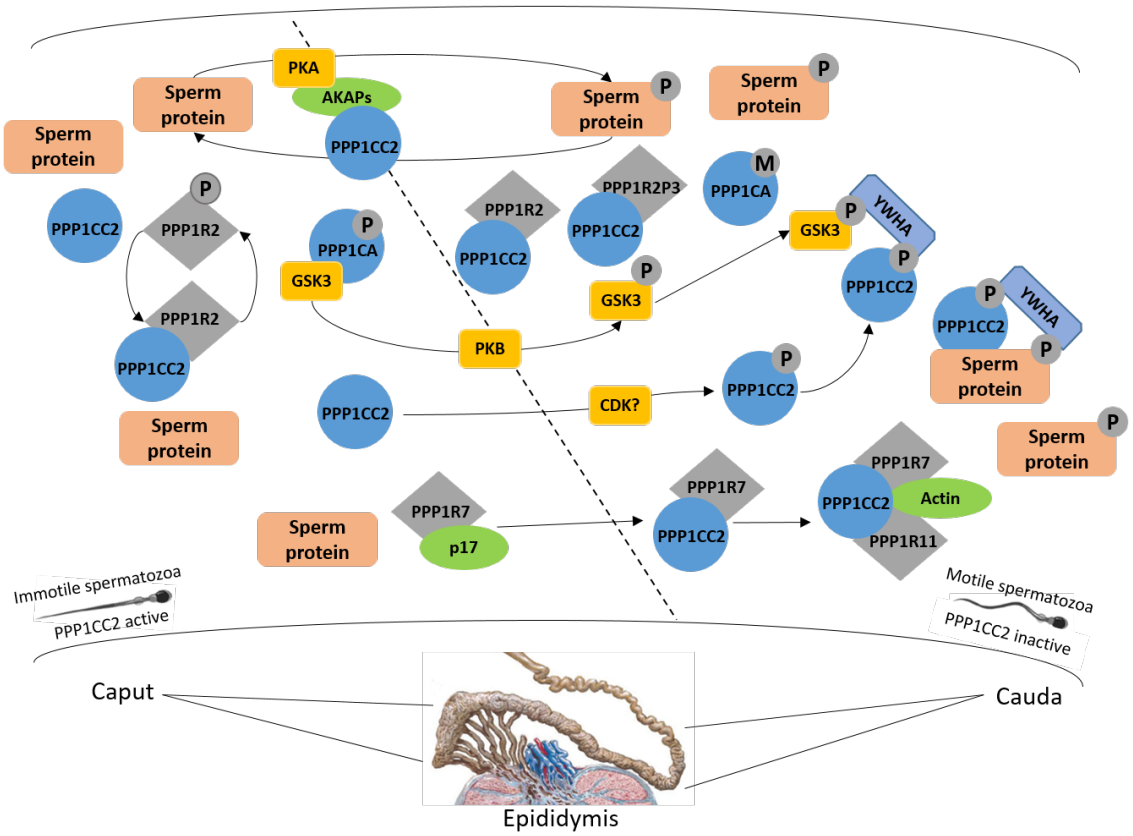

Figure 3 - Schematic representation of the role of PPP1CC2 in the regulation of sperm motility acquisition. AKAPs anchoring modulate PPP1CC2 and PKA activities regulating phosphorylation events. In caput epididymis, PPP2CA is phosphorylated and consequently active, which in turn dephosphorylated GSK3 that becomes active too. GSK3 phosphorylates PPP1R2 (I-2) which inhibits the interaction between PPP1R2 and PPP1CC2 resulting in active PPP1CC2, and consequently, immotile spermatozoa. PPP1R7 (sds22) is unable to inhibit PPP1CC2 since it is bound to p17. In caput epididymis, active PPP1 results in protein dephosphorylation and then immotile spermatozoa. In caudal epididymis, the inhibition of PPP2CA and the binding of Wnt to LRP6 receptor results in increasing of GSK3 serine phosphorylation leading to GSK3 inhibition. The inhibition of GSK3 leads to decrease of Thr73 PPP1R2 phosphorylation. Consequently, PPP1R2 binds PPP1. PPP1 is also bound to PPPP1R2P3 (I-2L) that cannot be phosphorylated by GSK3. A multimeric complex has been identified composed by PPP1CC2, PPP1R7, actin and PPP1R11 (I-3), where PPP1CC2 was inactive. Thus, PPP1 activity is inhibited leading to motile spermatozoa. Phosphorylated GSK3 and phosphorylated PPP1CC2 are bound to YWHA (14-3-3) in caudal sperm. P, phosphorylated; M, methylated. Adapted from [59].

1.1.1.2 PPP1CC2/PPP1R11/PPP1R7 Complex

PPP1R11 (I3), a human homologue of the t-complex expressed protein 5 (Tctex5) present in mouse [72], is a heat-stable PPP1 inhibitor protein [73] located in the head and principal piece of the tail (Figure 4). This protein has been linked to male infertility phenotypes of impaired sperm tail development and poor sperm motility [71,74]. PPP1R7 is a yeast sds22 homologue identified in caudal spermatozoa as a regulator of PP1CC2 activity [75–77]. In contrast, PP1CC2 and sds22 do not interact in caput bovine sperm. In male germ cells, PPP1CC2, PPP1R2, PPP1R7 and actin form a multimeric complex in which PPP1CC2 seems to be inactive [78]. Additionally, PPP1R7 has consensus sites for phosphorylation by GSK-3, protein kinase-A (PKA) and calmodulin dependent kinase II, all present in sperm [59]. It is possible that PP1CC2 activation and inactivation, due to its binding and dissociation from sds22, might be part of the mechanisms regulating motility and other sperm functions but its role needs to be further elucidated.

1.1.1.3 PPP1CC2/YWHA Complex

PPP1CC2 has at the C-terminus a consensus TPPR amino acid sequence containing a threonine residue (T320) that can be phosphorylated by cyclin-dependent kinases (CDKs) [79,80], like CDK2 [34]. The amount of phosphorylated PP1CC2 increases during sperm epididymal maturation and is located in equatorial region of the head and the principal piece of the tail [34]. In caudal spermatozoa, only phosphorylated PPP1CC2 exists. The regulation of PPP1CC2 by CDK2 could be achieved through the binding of PPP1CC2 to the bridging molecule 14-3-3 (YWHA) [81]. YWHA isoform is a highly conserved family of acidic proteins, expressed in many eukaryotic cells, that regulate processes such as cell cycle, apoptosis, protein trafficking, metabolism and transcriptional regulation of gene expression [71]. This protein, in mature spermatozoa, is present in the post-acrosomal region of the head and the principal piece [81] (Figure 4) and binds to PPP1CC2 when phosphorylated, regulating its catalytic activity, phosphorylation or interaction with other proteins [71]. GSK3 also binds to YWHA [82].

1.1.1.4 PPP1CC2/AKAP/PKA Complex

Several studies suggest that PPP1/AKAP/PKA complex is essential for sperm motility regulation. Cyclic AMP (cAMP) analogues and phosphodiesterase inhibitors increase the motility of mature spermatozoa. It has been proposed that elevated cAMP stimulates the phosphorylation of sperm proteins by PKA leading to increased motility [83]. Furthermore, anchoring of PKA through AKAPs to distinct intracellular sites in sperm is believed to be essential for regulating sperm motility since disruption of the AKAP–PKA interaction

results in motility arrest [84]. AKAPs function by target the cAMP-dependent PKA to various subcellular locations via the regulatory subunits of the kinase [85]. To date, more than 40 AKAPs have been identified, three of them associated with PPP1CC2 (AKAP220, AKAP3 and AKAP4) [85–87] in testis/sperm. AKAPs and PPP1CC2 are both present in the flagellum, so they might be involved in motility acquisition [22,86].

AKAP220/AKAP11 binds PKA and PPP1, inhibiting the phosphatase [88]. AKAP220 mRNA is expressed at high levels in human testis and in isolated human pachytene spermatocytes and round spermatids. In human germ cells and mature sperm, AKAP220 is located in the mid piece and associated with cytoskeletal structures [87]. The AKAP220 associated to the mid piece could serve to anchor PKA and/or PPP1CC2, regulating the contractile machinery in the sperm axoneme. It has also been showed that disruption of RII-AKAP interaction by peptides is responsible for the arrest of sperm motility [84].

AKAP3 (or AKAP 110) is a testis-specific protein found only in the fibrous sheath and located to the circumferential ribs of human sperm [23,85]. This protein binds to the RII subunit of PKA. AKAP3 binds to PDE4A (phosphodiesterase 4A cAMP specific) potentially controlling PKA activity [59]. Specific inhibitors of PDEs increase the motility of the cell, and PKA-anchoring inhibitor peptides arrest sperm motility [84].

AKAP4 (originally called AKAP82) is only expressed in testis and is the major protein in the fibrous sheath [85]. The transcription of this AKAP is initiated 20-22 days after birth and the mRNA is present in spermatids but not in pachytene spermatocytes [26]. A targeted disruption of the *Akap4* gene causing defects in mice sperm flagellum through the lack of fibrous sheath of the principal piece affecting male mice fertility was also demonstrated by Miki *et al*. [21]. Additionally, *Akap4* gene knockout in mice changes the activity and phosphorylation of PPP1CC2, as demonstrated by Huang and colleagues [89]. This suggests that AKAP4 is required to regulate the phosphorylation levels of PPP1CC2 in the principal piece of the spermatozoa.

These findings suggest that the PPP1CC2/AKAP/PKA complex is important for regulation of sperm motility and the loss of PPP1CC2-AKAP4 interaction results in immotile spermatozoa. Sperm-specific AKAPs seem to be a very directional target for the development of male contraceptives or for infertility therapeutics.

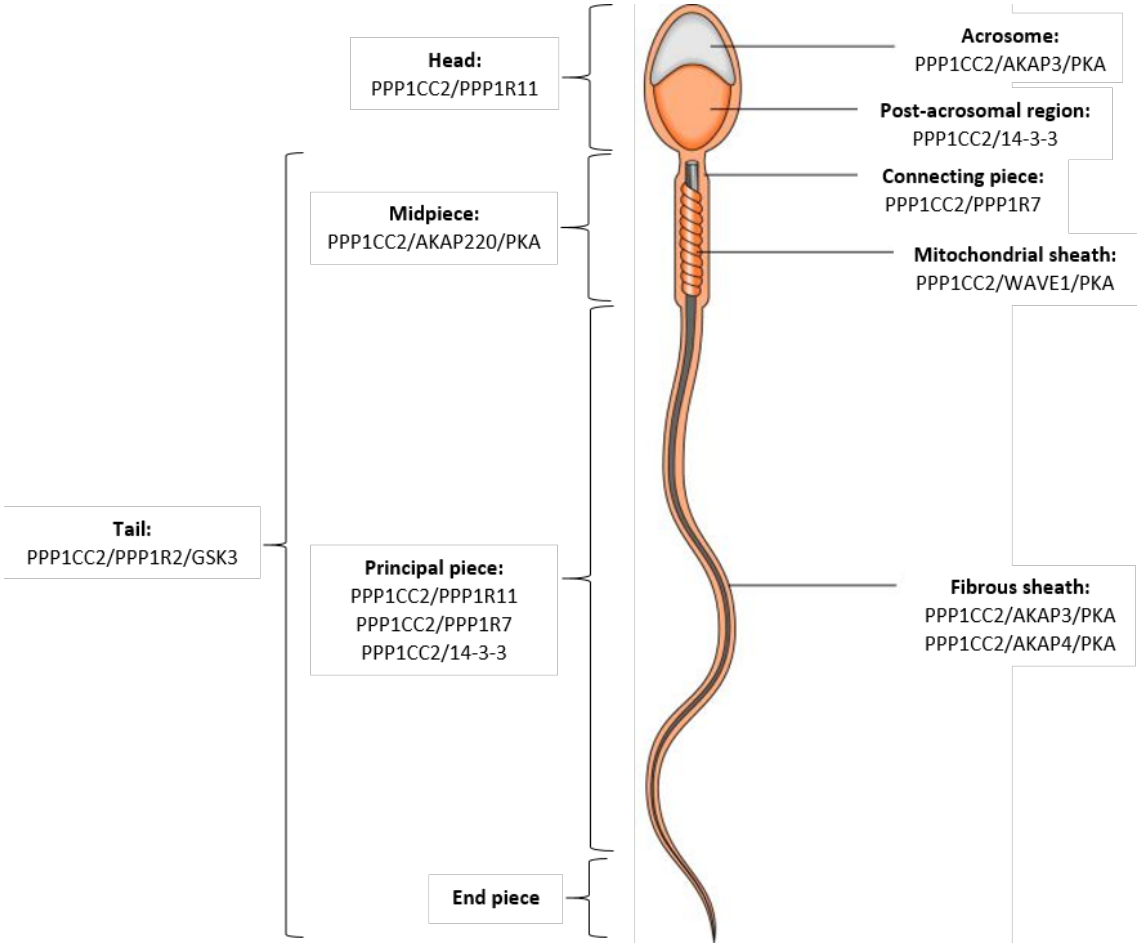

Figure 4 – Schematic representation of subcellular localization of protein phosphatase and interacting proteins (PPP1-PIP) complexes in spermatozoa. AKAP, A-kinase anchoring protein; GSK-3, glycogen synthase kinase-3; PKA, Protein kinase A. Adapted from [59].

1.5. Cell-Penetrating Peptides and their clinical potential

The cell uses different mechanisms, such as post-translation modifications (PTMs) and protein-protein interactions (PPI), to regulate its signal cascades. One of the most commons PTMs that occur in the cell is phosphorylation, corresponding to chemical alterations in the protein structure that change its structural conformation and the accessibility between enzymes and interacting proteins [90]. On the other hand, PPIs are defined as “physical contacts with molecular docking between proteins that occur in a cell or in a living organism in vivo” [91]. These interactions can be permanent, when a stable complex is formed, or transitory, when is involved in signaling pathways. Not all possible interactions occur in any cell at any time. In fact, interactions depend on the biological context, such cell type, cell cycle phase, development stage, environmental conditions, protein modifications, presence of cofactor and presence of other binding partners [92].

In the past two decades, PPI have emerged as promising drug targets and the field is evolving fast [93]. Several approaches have been used to modulate PPIs, in particular those based on the use of small organic molecules derived from natural compounds or organic synthesis [94]. Recombinant proteins/antibodies and peptides can explore large surfaces and, thus, being excellent PPI modulators. Peptides in particular have several advantages like: (i) adaptability to larger surfaces due to their flexibility, (ii) easy modularity, which increases structural diversity allowing for higher selectivity and potency, (iii) accumulation only in a minor extent in tissues and (iv) biocompatibility, which means low toxicity in humans [95]. However, peptides are difficult to convert into oral drugs, they are not metabolically stable undergoing rapid removal by hepatic and renal clearance, they do not cross physiological barriers easily and they have poor oral bioavailability, due the digestion by proteases for example. Fortunately, peptides can be easily synthetized and modified to improve their stability, permeability and bioavailability [96].

Cell-penetrating peptides (CPPs) are a class of cellular delivery vectors and are reliable vehicles for the intracellular delivery of therapeutic agents [96]. CPPs are short peptide sequences, consisting of less than 30 amino acids in length and often carry a positive charge, that can pass through the cellular membrane and deliver different types of cargo that are usually unable to cross an intact lipid barrier [94,97] (Figure 5).

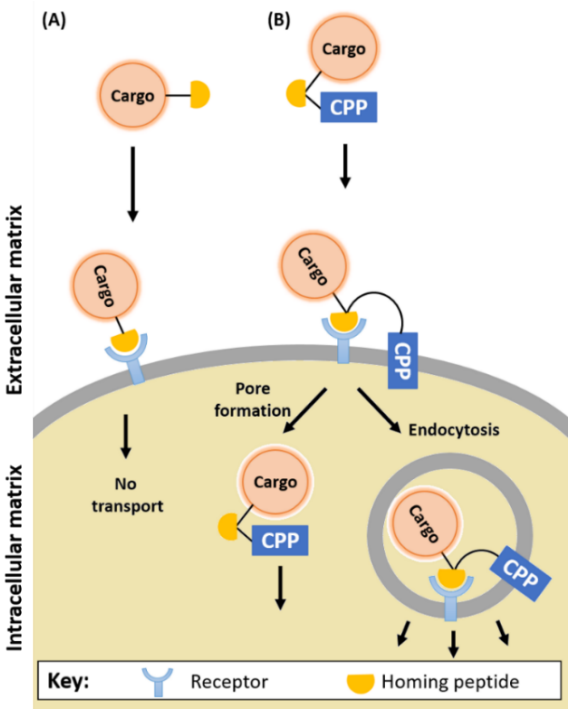

Figure 5 – Principle of cell-penetrating peptide targeting and delivery. (A) A homing peptide (HP) has no inherent internalization properties and only delivers its cargo to specific cell-surface receptors. (B) A HP conjugated with cell-penetrating peptides (HP-CPP) undergoes receptor binding and undergoes cargo internalization via endocytosis or pore formation. Adapted from [98].

The peptides are usually classified according to their physicochemical properties into cationic, amphipathic, hydrophobic and anionic categories [97,99] or according to their origin in: 1) a polypeptide motif derived from natural proteins with penetrating functions, 2) an artificially designed and synthetic polypeptides which are optimized as molecular-internalizing vectors or 3) a chimeric sequence [94]. The first two CPPs described, penetratin and Tat peptide, are cationic stretches of amino acids identified in the primary sequences of both insect- and virally-encoded transcription factors, respectively [96]. These polycationic CPP motifs confer their native proteins the capacity to cross biological membranes to achieve their role as transcriptional activators. Similar CPP sequences have been also identified in several human proteins [96]. Today, the class of CPPs includes numerous amino acid sequences that can be broadly divided into tissue-specific and non-tissue specific peptides [100,101] (Table 1). The identification of intrinsically bioactive CPPs emphasizes the tremendous clinical potential of CPP technologies [102]. In terms of clinical applications, CPP can potentially be used to deliver a wide range of therapeutic moieties, including small molecules, liposomes, nanoparticles and biopharmaceuticals including oligonucleotides, peptides and proteins [102,103].

Table 1 – Examples of some common cell-penetrating peptides and their applications.

Name	Sequence	Source	Cargo
Cationic			
Tat [104]	GRKKRRQRRRPPQ	HIV Tat protein	Gene vectors, proteins, peptides, label
Penetratin [105]	RQIKIWFQNRRMKWKK	Antennapedia homeodomain	Gene vectors, proteins, peptides, label
Polyarginine [106]	Rn (n =6–12)		Gene vectors, liposomes, label
8-Lysine [107]	KKKKKKKK		
PTD-4 [108]	YARAAARQARA		
PTD-5 [108]	RRQRRTSKLMKR		
Oct4 [109]	DVVRVWFCNRRQKGKR	Oct4 protein	
WT1-pTj [110]	KDCERRFSRSDQLKRHQRRHTGVKPFQ	Wilms tumor protein 1	
DPV3 [111]	RKKRRRESRKKRRRES	Heparin binding protein	Protein, label
M918 [112]	MVTVLFRRLRIRRACGPPRVRV	Tumor suppressor protein p14ARF	Label Proteins Proteins and nucleic acids
Hydrophobic			
Transportan [113]	GWTLNSAGYLLGKINLKALAALAKKIL	Galanin and mastoparan	Gene vector, label
MAP [114]	KLALKLALKALKAALKLA		Label
TP10 [115]	AGYLLGKINLKALAALAKKIL	Galanin and mastoparan	
Pep1 [116–118]	KETWWETWWTEWSQPKKKRKV	SV 40 NLS and a hydrophobic domain	Proteins, gene vectors
KW [119]	KRKRWHW		Small molecules
Amphipathic			
Azurin p18 [120]	LSTAADMQGVVTDGMASG	Azurin	
Azurin p28 [121]	LSTAADMQGVVTDGMASGLDKDYLKPDD	Azurin	
hCT18-32 [122]	KFHTFPQTAIGVGAP	Calcitonin	
pVEC [123]	LLIILRRRIRKQAHAHSK	VE-cadherin	Proteins, fluorophores
VP22 [124,125]	NAATATRGRSAASRPTQRPRAPARSASRP RRPVQ	Herpes simplex virus envelope protein	
C105Y [126–128]	CSIPPEVKFNKPFVYLI	α1-Antitrypsin	Gene vector, peptide, liposome
JTS1 [129]	GLFEALLELLESLWELLLEA		
VT5 [130]	DPKGDPKGVTVTVTVTVTGKGDPKPD		
Mastoparan [131]	INLKALAALAKKIL		

Name	Sequence	Source	Cargo
Mitoparan [131]	INLKKLAKL(Aib)KKIL		Voltage-dependent anion channel
CPPs-tissue specific			
CTP [132]	APWHLSSQYSRT	Phage display	
K5-FGF [133]	AAVALLPAVLLALLP	Kaposi fibroblast growth factor	Peptides, antibodies
HAP-1 [134]	SFHQFARATLAS	Phage display	
293P-1 [135]	SNNNVRPIHIWP	Phage display	
Others			
Nosangiotide [102]	RKKTFKEVANAVKISA		
Camptide [102]	RKLTTIFPLNWKYRKALSLG		
Cyt c $^{77\text{-}101}$ [136]	GTKMIFVGIKKKEERADLIKKA	Cytochrome c	

Two approaches are generally applied when CPPs are employed as delivery vectors: covalent conjugation (sychnologic pattern) and physical complexation (rhegnylogic pattern) [97]. A sychnologically organized CPP could include CPP joined to a bioactive peptide in which every amino acid side-chain is a *message* pharmacophore. The linker joining these two distinct peptides as a tandem structure can be a conventional peptide bond, a disulphide or other covalent structure. In the rhegnylogic organization the pharmacophores for penetration (address) and bioactivity (message) are discontinuously distributed within a single peptide [102] (Figure 6).

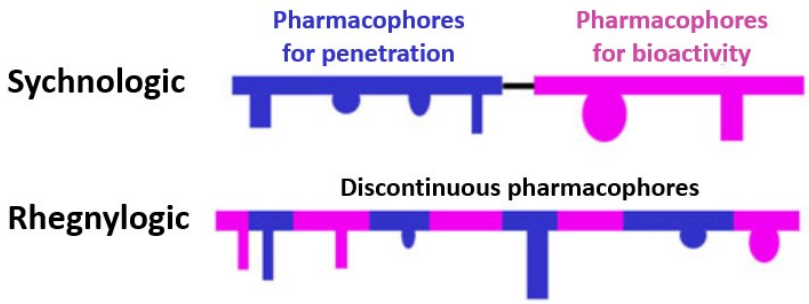

Figure 6 - Bioactive peptides can be delivered as a sychnologically-organized chimera conjugated to CPPs or as a rhegnylogic organization. In this conceptual diagram the pharmacophores responsible for penetration are illustrated in blue, whereas those conferring bioactivity are colored purple. Adapted from [102].

CPP internalization may be achieved by both direct plasma membrane translocation and energy-dependent endocytic mechanisms that depends on cell type, CPP concentration and size and nature of the conjugated cargo [96,99]. Several types of endocytosis have been demonstrated for different peptides, including caveolar, clathrin-mediated and micropinocytosis [99]. The mechanism of uptake is highly dependent on the type of cargo, making it difficult to predict which penetrating peptide should be selected in each case. The CPP technology have numerous advantages which include low toxicity, more precise target-specificity and routes of administration that may be relatively non-invasive [96,98]. Compared with other traditional techniques, such as microinjection or electroporation,

CPPs do not destroy the integrity of cell membranes and are considered high efficient and safe [94] and also can be vectors for the delivery of peptides across epithelia and the blood-brain barrier [97].

CPP-mediated delivery of peptides and proteins has been successfully applied to target cancer, muscular dystrophy, cardiology, prion diseases, to treat systemic and local inflammations resulting from invasion by pathogens or a chemical or physical injury and have also been applied to induce generation of pluripotent stem cells as a safer strategy than the classical method involving introduction of viral genetic material [97,137].

Recently Jones and colleagues demonstrated that CPPs are able of translocate into the sperm cell and modulate sperm physiology and function without affecting its viability and motility [138]. Another study demonstrates that CPPs accumulate differentially at distinct structural compartments within spermatozoa [139]. In fact, Tat accumulates within the spermatozoa head, including the acrosome, Mitoparan (MitP) demonstrates a propensity for mitochondrial localization and C105Y accumulates in all structures of sperm except the interior head and acrosome [139].

In the present study, three peptide sequences derived from (i) the 22 amino acid C-terminus of the human PPP1CC2 (303KPNATRPVTPPRVASGLNPSIQKASNYRNNTVLY336) [PPP1CC2-CT], (ii) the region including the PPP1 binding motif (40KVICF44) of the human AKAP4 (33GQQDQDRKVICFVDVSTLNV52) [AKAP4-BM] and (iii) a mutated homologue (33GQQDQDRAAAAAVDVSTLNV52) [AKAP4-BM M] previously synthesized using microwave-assisted solid-phase peptide synthesis were used. These endogenous sequences and structural analogues were coupled to penetratin (RQIKIWFQNRRMKWKK), an inert CPP (Table 2).

Table 2 - Peptide sequences, abbreviation and molecular masses. Underlined, penetratin (CPP); **Bold**, PPP1 binding motif (pattern: [RK]-X(0,1)-[VI]-{P}-[FW]).

Peptide designation	Abbreviation	Peptide sequence	Mass (g/mol)
PPP1CC2 C-terminal[1]	PPP1CC2-CT	NH2-RQIKIWFQNRRMKWKKKPNATRPVTPPRVASGLNPSIQKASNYRNNTVLY-H	5953,0124
AKAP4 binding motif	AKAP4-BM	H-KKWKMRRNQFWIKIQRVNLTSVAV**FCIVK**RDQDQQG-NH2	4448,3148
AKAP4 binding motif mutant	AKAP4-BM M	H-KKWKMRRNQFWIKIQRVNLTSVAV**AAAAA**RDQDQQG-NH2	4212,9217

[1]The last amino acid of PPP1CC1 C-terminus (glutamic acid) was excluded due to its negative charge.

1.6. *Aims*

World's population has been rising and it is expected that it will reach 9-10 billion by 2050. This population growth is a leading cause of environmental degradation and human suffering from poverty [140]. Despite the currently available contraceptive methods, the number of unintended pregnancies worldwide is still high. Contraceptive nonuse, incorrect use and failure result in over than 20% of pregnancies ending in abortion [141,142] and unplanned children are often exposed to poverty and neglect environments. Unplanned birth may also have serious health, economic and social consequences for families [143]. These statistics reflect the need for new contraceptive methods to overcome the problem of unintended pregnancy, abortion and uncontrolled fertility. Compared with female, male contraceptive methods are few and underused. According the United Nations, in 2015, only 12% of couples used condom, being preferentially used female contraceptives such as pill and intra-uterine device. The development of new contraceptives has focused upon hormonal modulation, however, this technology had several side effects [140,144,145]. The mechanism of spermatozoa motility acquisition is a perfect target for a new male contraceptive since normal hormone and spermatozoa production occur and only the post-testicular sperm maturation is affected.

Thus, the main goal of this study is to modulate protein complexes in spermatozoa and, consequently, sperm motility using cell-penetrating peptides that specifically interact with non-hormonal targets selectively expressed in testis and sperm. To that, we proposed to:

1. Evaluate the concentration- and time-dependent intracellular uptake of the cell-penetrating peptides in spermatozoa;
2. Evaluate the impact of the cell-penetrating peptides on spermatozoa motility;
3. Evaluate the disruptive potential of the AKAP4-BM peptide on the AKAP4-PPP1CC2 interaction;
4. Characterize the interactome of the PPP1CC2-CT peptide in spermatozoa.

2. Material and Methods

Experimental procedures were performed in Signal Transduction Laboratory, Institute for Research in Biomedicine (iBiMED), University of Aveiro (Aveiro, Portugal). The details of the solutions used in this thesis are stated in the Supplementary Table 1.

2.1. Sample processing

This study was approved by the Ethics and Internal Review Board of the Hospital Infante D. Pedro E.P.E. (Aveiro, Portugal) and was conducted in accordance with the ethical standard of the Helsinki Declaration. Ejaculated human semen samples from volunteer donors were collected by masturbation into a sterile container. All donor signed an informed consent allowing the use of the samples for scientific proposes. Basic semen analysis was conducted in accordance with World Health Organization (WHO) guidelines [146] and only normal sperm samples were used. Briefly, after complete liquefaction of the semen samples at 37˚C, during approximately 30 minutes, a macroscopic examination was performed. The microscopic examination included the analysis of spermatozoa motility, concentration and morphology. All microscopy analyses were performed using a Zeiss Primo Star microscope (Carl Zeiss AG, Germany). The results of basic sperm analysis were detailed in Supplementary Table 2. Frozen semen from bulls was obtained from LusoGenes, LDA (Aveiro, Portugal). Bovine semen was thawed in a 37°C water bath for 1 min. Human and bovine spermatozoa were isolated and washed three times from seminal plasma by centrifugation (600g for 10 min at room temperature) using ALLGrad Wash medium (LifeGlobal, Brussels, Belgium). Pellet was re-suspended in medium to a final concentration desired and incubated at 37°C with 5% CO_2 until the appropriated treatments were added. The concentration of sperm cells after the washing procedures was assessed using the Sperm Class Analyzer CASA System (Microptic S L, Barcelona, Spain) with SCA® v5.4 software. Samples and controls (2 µl) were loaded into individual chambers of Leja Standrat Count 8 chamber slide 20 µm depth (Leja Products B. V., The Netherlands) which were pre-heated at 37°C.

2.2. Quantitative uptake analysis

For the temporal-dependent quantitative uptake analysis of the competition peptides, 5 million of bovine spermatozoa were incubated with 5 µM TAMRA-labeled peptides for 15, 30 and 60 min at 37°C in a humidified atmosphere of 5% CO_2. For the

concentration-dependent quantitative uptake analysis of the competition peptides, 5 million of bovine spermatozoa were incubated with 5 µM, 7,5 µM and 10 µM TAMRA-labeled peptides for 15 min at 37°C in a humidified atmosphere of 5% CO_2. In both cases, after incubation with the peptides, the peptide containing solution was removed by centrifugation (600g for 10 min) and the pellet was washed two times with 200 µl of phosphate buffered saline (PBS) (600 g for 5 min). Cells were detached with 300 µl of 1% (wt/vol) trypsin at 37°C, collected by centrifugation at 3000 g and lysed in 300 µL 0.1 M NaOH for 2h on ice. 250 µL of each cell sample lysate were transferred to a black 96-wells plate and analyzed using an Infinite® 200 PRO (Tecan, Switzerland) (λAbs 544 nm/λEm 590 nm).

2.3. Motility assays

To perform the motility assays, 20 million of sperm cells per treatment/well were used in a final volume of 250 µl. Sperm cells were incubated with 5 µM and 10 µM of the peptides (PPP1CC2-CT, AKAP4-BM and AKAP4-BM M). Control samples included sperm cells in medium. Samples and controls were incubated during 15 min at 37°C in a humidified atmosphere of 5% CO_2. The influence on sperm motility parameters was assessed using the Sperm Class Analyzer CASA System (Microptic S L, Barcelona, Spain) with SCA® v5.4 software. Samples and controls (2 µl) were loaded into individual chambers of Leja Standart Count 8 chamber slide 20 µl depth (Leja Products B V, The Netherlands) pre-heated at 37ºC. This temperature was maintained while at least 700 sperm cells per measurement were evaluated. Each peptide was testes on samples from three different bulls and all the conditions were performed in triplicate.

2.4. Antibodies

Homemade anti-PPP1CC2 antibody was used for Western Blot and immunoprecipitation studies. Primary antibodies used for Western Blot are summarized in Table 3. The infrared IRDye®680RD anti-rabbit (926-68071) and IRDye®800CW anti-mouse (926-32210) secondary antibodies (1:5000) were obtained from LI-COR Biosciences (Lincon, NE, USA).

Table 3 – Primary antibodies used for Immunoblot.

Antibody	Host	Dilution	Molecular Weight (kDa)	Reference	Supplier
Anti-PPP1CC2	Rabbit	1:2000	~37	G502	Homemade
Anti-AKAP4	Rabbit	1:300	~94	Ab123415	Abcam
Anti-AKAP4	Mouse	2,5 µg/ml	~94	ab56551	Abcam
Anti-GPX4	Rabbit	1:1000	~20	ABC269	Millipore
Anti-β-tubulin	Mouse	1:2000	-50	32-2600	Invitrogen

2.5. Co-immunoprecipitation of PPP1CC2

For the detection of PPP1CC2/AKAP4 interaction, 40 million of human sperm cells (volunteer 1, Supplementary Table 2) per condition were lysed in 1000 µl of 1x RIPA buffer (0.5 M Tris-HCl, pH 7.4, 1.5 M NaCl, 2.5% deoxycholic acid, 10% NP-40, 10 mM EDTA) (Millipore Iberica S.A.U., Madrid, Spain) supplemented with protease inhibitor (1 mM PMSF) for 30 minutes on ice and centrifuged at 16000 g for 15 min at 4ºC.

For the competition assays, 20 million of human (volunteers 2 and 3, Supplementary Table 2) or bovine spermatozoa were incubated with 10 µM and 50 µM of AKAP4-BM and AKAP4-BM M peptides for 15 min. The peptide containing solution was removed (600g for 5 min) and sperm cells were lysed in 1000 µl 1x RIPA buffer (0.5 M Tris-HCl, pH 7.4, 1.5 M NaCl, 2.5% deoxycholic acid, 10% NP-40, 10 mM EDTA) (Millipore Iberica S.A.U., Madrid, Spain) supplemented with protease inhibitor (1 mM PMSF) for 1h on ice and centrifuged at 16000 g for 10 min at 4ºC. Ninety percent of the supernatant was used for the subsequent steps (sperm soluble fraction). Ten percent of the soluble fraction was saved and the pellet (insoluble fraction) was re-suspended in 1000 µl 1% sodium dodecilsulfate (SDS) (sperm insoluble fraction).

RIPA supernatant extracts were pre-cleared using 20 µl of Dynabeads® Protein G (Life Technologies AS., Madrid, Spain) per condition, during 30 min at 4ºC with rotation. An indirect co-immunoprecipitation approach was performed using 2 µg of homemade rabbit anti-PPP1CC2 overnight at 4ºC with rotation. 100 µl of beads were posteriorly added to the extracts and incubated 2 hours at 4ºC with rotation. After incubation, the supernatant was removed to a new microtubule and stored (unbound IP fraction) and the beads were washed two times with 500 µl PBS during 15 min at 4ºC with rotation. After washing, the beads were re-suspended in 1x loading buffer and boiled for 5 minutes. The eluted fraction was then collected (IP fraction).

2.6. Co-immunoprecipitation of biotinylated PPP1CC1-CT peptide

To identify the interactome of the PPP1CC2-CT peptide in human spermatozoa, a co-immunoprecipitation of the biotinylated PPP1CC2-CT peptide was performed. 15 million of human sperm cells (volunteers 4 to 6, Supplementary Table 2) were incubated with 5 µM of biotinylated PPP1CC2-CT peptide for 15 min at 37°C in a humidified atmosphere of 5% CO_2. The peptide containing solution was removed (600g for 15 min) and sperm cells were lysed in 250 µl of 1x RIPA buffer (0.5 M Tris-HCl, pH 7.4, 1.5 M NaCl, 2.5% deoxycholic acid, 10% NP-40, 10 mM EDTA) (Millipore Iberica

S.A.U., Madrid, Spain) supplemented with protease inhibitor (1 mM PMSF) for 30 min on ice and centrifuged at 16000g for 15 min at 4ºC. Ninety percent of the supernatant was used for the subsequent steps (sperm soluble fraction). Ten percent of the soluble fraction was saved and the pellet (insoluble fraction) was re-suspended in 250 µl 1% SDS (sperm insoluble fraction). 50 µl per condition of Dynabeads® M-280 Streptavidin (Life Technologies AS., Madrid, Spain) were added to the RIPA supernatant extracts and incubated for 30 min at room temperature with gentle rotation. After incubation, the supernatant was removed to a new tube and stored (unbound IP fraction) and the beads were washed three times with 1 ml 1X PBS (for western blot) or with 1 ml trypsin digestion buffer (20 mM Tris-HCl pH 8.0, 2 mM CaCl2) (for LC-MS/MS). After washing, the beads were re-suspended in 30 µl LB 1X (for western blot) or in 150 µl trypsin digestion buffer (20 mM Tris-HCl pH 8.0, 2 mM CaCl2) (for LC-MS/MS at VIB Proteomics Core, Gent, Belgium) and stored at -20°C.

2.7. Western Blotting

The extracts were resolved by 10% or 15% SDS-polyacrylamide gel electrophoresis (PAGE) and proteins were electrotransferred onto nitrocellulose membranes. The gel was run at 200 V and electrotransferred at 200 mA for 2 hr. Non-specific protein-binding sites on the membrane were blocked with 5% bovine serum albumin (BSA) in Tris-buffered saline containing 0.1% Tween 20 (TBST) for 1h. The blots were then washed with TBST and incubated with primary antibodies (rabbit anti-PPP1CC2 or anti-β-tubulin for 1h at room temperature and rabbit anti-AKAP4, mouse anti-AKAP4 or rabbit anti-GPX4 overnight at 4ºC). After the incubation, the blots were washed three times for 10 min each with TBST and then incubated with the appropriate secondary antibody for 1h at room temperature. Blots were washed three times for 10 min with TBST and once with Tris-buffered saline (TBS: 25 mM Tris-HCl, pH 7.4, 150 mM NaCl) and immunodetected using the Odyssey Infrared Imaging System (LI-COR® Biosciences, US).

2.8. Cell culture

HeLa cells were cultured in Dulbecco's Modified Eagle's Medium (DMEM) (Sigma) medium supplemented with 10% Fetal Bovine Serum (FBS) and antibiotics (1% penicillin/streptomycin mixture). Cells were grown in 10 cm plates in a 5% CO_2 humidified incubator at 37ºC and sub cultured every 2-3 days.

2.9. Cell transfection

Lipofectamine®2000 was used for transfection of HeLa cells using the pCMV6-AC-GFP-AKAP4 or pEGFP-N1 expression vectors. One day before transfection, 1 x 10^5 cells were plated in 10 ml of DMEM medium supplemented with 10% FBS without antibiotics so they were 70-90% confluent at the time of transfection. For each transfection sample in 10 cm plates the DNA/lipofectamine complexes were prepared as follows: 50 µl of lipofectamine® 2000 were diluted in 1450 µl of Opti-MEM®I medium without serum and added to 20 µg of plasmid DNA previously diluted in 1500 µl of the same medium. The mixture was allowed to complex for 20 min at RT and then 3 ml of the complex were added to each plate containing cells and medium mixing gently by rocking the plate back and forth. 24h after incubation at 37ºC in a CO_2 incubator, transfected cells were washed twice in 1X PBS and cell extracts were prepared. 1.5 ml of SDS 1% were added to each plate and cells were collected with a scrapper. Lysed cells were centrifuged at 16 000g for 20 min and sonicated three times for 10 sec. Extracts were mass normalized using the bicinchoninic acid (BCA) assay (Fisher Scientific, Loures, Portugal). Sample were prepared to be assayed with 5 µL of each sample plus 20 µL of 1% SDS. Standard protein concentrations were prepared as described in Supplementary Table 3. Samples and standards were prepared in duplicate. The BSA stock solution used had a concentration of 2 mg/ml. The Working Reagent (WR) was prepared by mixing BCA reagent A with BCA reagent B in the proportion of 50:1. Then, 200 µl of WR was added to each well (standards and samples) and the plate was incubated at 37 ºC for 30 min. Once the tubes cooled to RT the absorbance was measured at 562 nm using an Infinite® 200 PRO (Tecan, Switzerland). A standard curve was obtained by plotting BSA standard absorbance *vs* BSA concentration, and used to determine the total protein concentration of each sample.

2.10. Membrane overlay

HeLa cells extracts were resolved by 10% SDS-PAGE and proteins were electrotransferred onto nitrocellulose membranes. 30 µg of protein were loaded per condition/well. The gel was run at 200 V and electrotransferred at 200 mA for 2 hr. The membranes were cut and only the top part were overlaid with: (i) 10 pmol purified PPP1CC2 and 50 pmol AKAP4-BM peptide; (ii) 10 pmol purified PPP1CC2 and 50 pmol AKAP4-BM M peptide; (iii) 10 pmol purified PPP1CC2 and (iv) 10 pmol purified PPP1CC2 and 25 pmol I-2. The incubations were performed in microtubes. The

membranes were blocked with 3% BSA in TBS for 30 min at room temperature. The purified PPP1CC2, the peptides (AKAP4-BM and AKAP4-BM M) and the I-2 were added to 1 mL of 3% BSA in TBS and allowed to incubate 15 min at 4ºC with gentle rotation. After blocking, the membranes were incubated with the corresponding conditions for 2 hours at room temperature with slow agitation. The membranes were then washed twice with TBST 1X for 10 min to remove the excess of protein and peptide and incubated with homemade rabbit anti-PPP1CC2 antibody (1:2000) for 1h at room temperature. After the incubation, the blots were washed three times for 10 min each with TBST and incubated with an Infrared IRDye-labeled anti-rabbit specific antibody for 1h at room temperature. Blots were washed three times for 10 min with TBST and once with TBS and immunodetected using the Odyssey Infrared Imaging System (LI-COR® Biosciences, US).

For loading control the bottom part of the membranes were incubated with Ponceau S. solution for 15 min at room temperature with slow agitation. The membranes were washed with distilled water until the protein bands were well defined and analyzed using the densitometer GS-800. To remove the staining, the membranes were washed with TBST 1X. The bottom part of the membranes was also blocked with 3% BSA in TBST-1X for 30 min and immunoblotted with mouse anti-β-tubulin (1:2000) for 1h at room temperature. Pixel intensity was quantified using Quantity One ® software. The intensity from an empty lane within each membrane was subtracted from all signals and all data was normalized to the Ponceau S. control.

2.11. Bioinformatic analysis

The data obtained by mass spectrometry was subjected to an extensive bioinformatic analysis. For the identification of testis/sperm enriched/specific proteins, cellular and subcellular localization proteins were searched against Human Protein Atlas (HPA), a tissue expression database. The criteria used in the database were set for a maximum stringency to identify the tissue-specific protein with a high confidence level. The Uniprot database was used to classify the proteins according their molecular function and biological process associated. Proteins associated with defects in male fertility or a functional/morphological defect in the male reproductive system were obtained from three databases: Diseases (http://diseases.jensenlab.org/Search), DisGeNET (http://www.disgenet.org/web/DisGeNET/menu;jsessionid=1q3ipxj2id1gbp3r47hkto884) and MGI (http://www.informatics.jax.org/).

3. Results

3.1. Peptides translocate into bovine spermatozoa at different rates

Quantitative analysis of the uptake efficacies in bovine spermatozoa demonstrated that the peptides tested have different translocation rates (Supplementary Table 4). AKAP4-BM internalized very efficiently, having the highest intracellular translocation efficacy of the three peptides tested, while AKAP4-BM M internalized less efficiently resulting in reduced fluorescent signal (Figure 7).

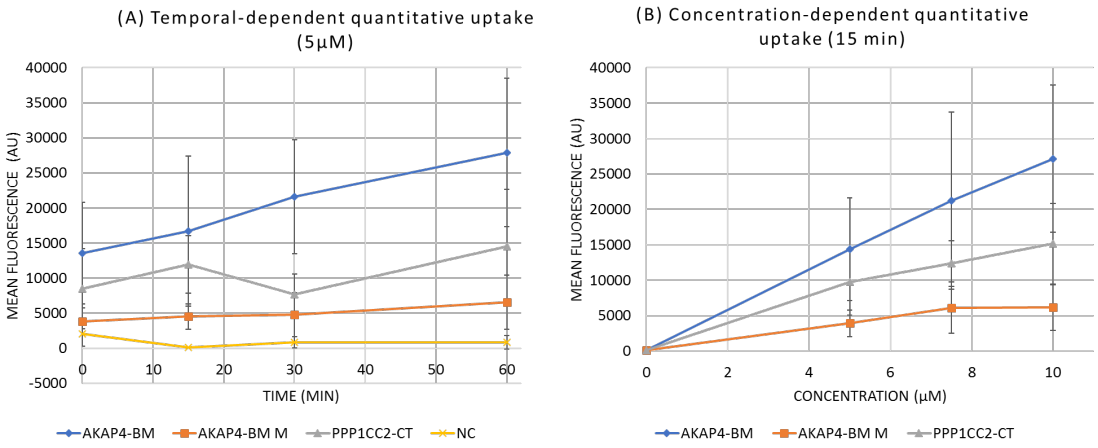

Figure 7 - Quantitative analysis of peptide translocation into bovine spermatozoa. (A) Temporal-dependent intracellular uptake of TAMRA-labeled peptides into bovine spermatozoa. Bovine spermatozoa were incubated with TAMRA-labeled CPP (5 µM) at 37ºC for the times indicated. (B) Bovine spermatozoa were incubated with 5 µM, 7,5 µM and 10 µM of TAMRA-labeled peptides for 15 min at 37ºC. The experiments were performed in triplicated in three different bulls. Data are expressed as mean fluorescence ± s.e.m.

At time zero, corresponding to the addition of the peptides to spermatozoa and immediate washing to remove the peptide containing solution, some peptide already entry in the sperm cells, revealing that peptides rapidly translocate into bovine spermatozoa. The amount of AKAP4-BM M peptide entering cells does not increase with time while AKAP4-BM and PPP1CC2-CT peptides uptake increased with time (Figure 7, A). However, it was observed that at 30 min of incubation with PPP1CC2-CT peptide the amount of peptide inside the sperm cells was less than at 15 min and 1h. This unexpected result can be explained by methodological errors.

Incubations with different concentrations of the competitive peptides were tested at 15 min in bovine spermatozoa and the intracellular translocation was evaluated (Figure 7, B and Supplementary Table 5). Exposure of bovine spermatozoa to increasing concentrations of AKAP4-BM peptide was followed by increasing intracellular translocation of the peptide. Similar results were found for PPP1CC2-CT and AKAP4-

BM M peptides, however, with 7,5 µM of the AKAP4-BM M peptide the intracellular quantity of the peptide starts to stabilize.

3.2. Impact of the peptides on sperm motility

Bovine spermatozoa were exposed to different extracellular peptide concentration (5 µM and 10 µM) and motility parameters were accessed at 15 minutes (Supplementary Table 6 to Supplementary Table 8) using the Sperm Class Analyzer CASA System (Microptic S L, Barcelona, Spain) with SCA® v5.4 software (Figure 8). Negative controls were performed in the absence of peptides.

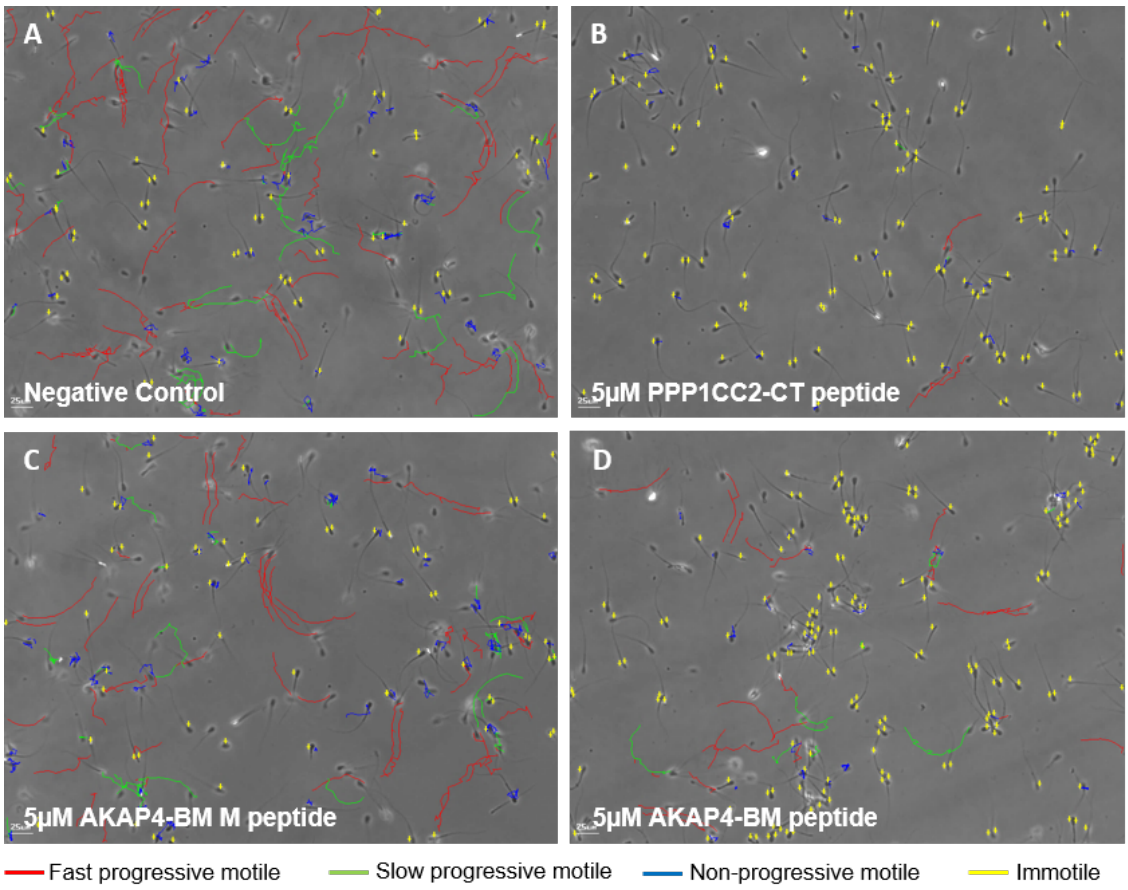

Figure 8 – Example of the assessment of motility using the Sperm Class Analyzer CASA System (Microptic S L, Barcelona, Spain) with SCA® v5.4 software. At least 700 sperm cells per measurement were evaluated. Negative control without the peptides was performed (A). Samples treated with 5 µM of PPP1CC2-CT peptide showed more immotile spermatozoa (B) when compared to negative control. When compared with mutated AKAP4-BM peptide (AKAP4-BM M) (C) and with negative control (A), sperm cells treated with AKAP4-BM peptide (D) also showed reduced motility. Images are representative from three independent experiments. Red, fast progressive motile spermatozoa; Green, slow progressive motile spermatozoa; blue, non-progressive spermatozoa; yellow, immotile spermatozoa.

3.2.1. PPP1CC2-CT peptide

After exposure of bovine spermatozoa to 5 μM of PPP1CC2-CT, a significantly reduction in fast (from 29,5±7,8% to 14,5±6,9%) and slow progressive motility (from 9,9±4,4% to 5,9±2,2%) was observed comparing with negative control. Incubation of bovine spermatozoa with 10 μM of the same peptide induced significant reduction in fast progressive motility (from 29,5±7,8% to 15,0±7,8%) but not in slow progressive motility. On the other hand, immotile spermatozoa increased with both 5 μM (from 37,3±9,6% to 58,1±9,3%) and 10 μM (from 37,3±9,6% to 50,5±13,3%) PPP1CC2-CT. No significant alterations were observed in non-progressive motility (Figure 9).

The concentrations tested (5 μM and 10 μM) had similar results for all the parameters, except for slow progressive motility, suggesting that there was no concentration-dependent effect of the PPP1CC2-CT peptide.

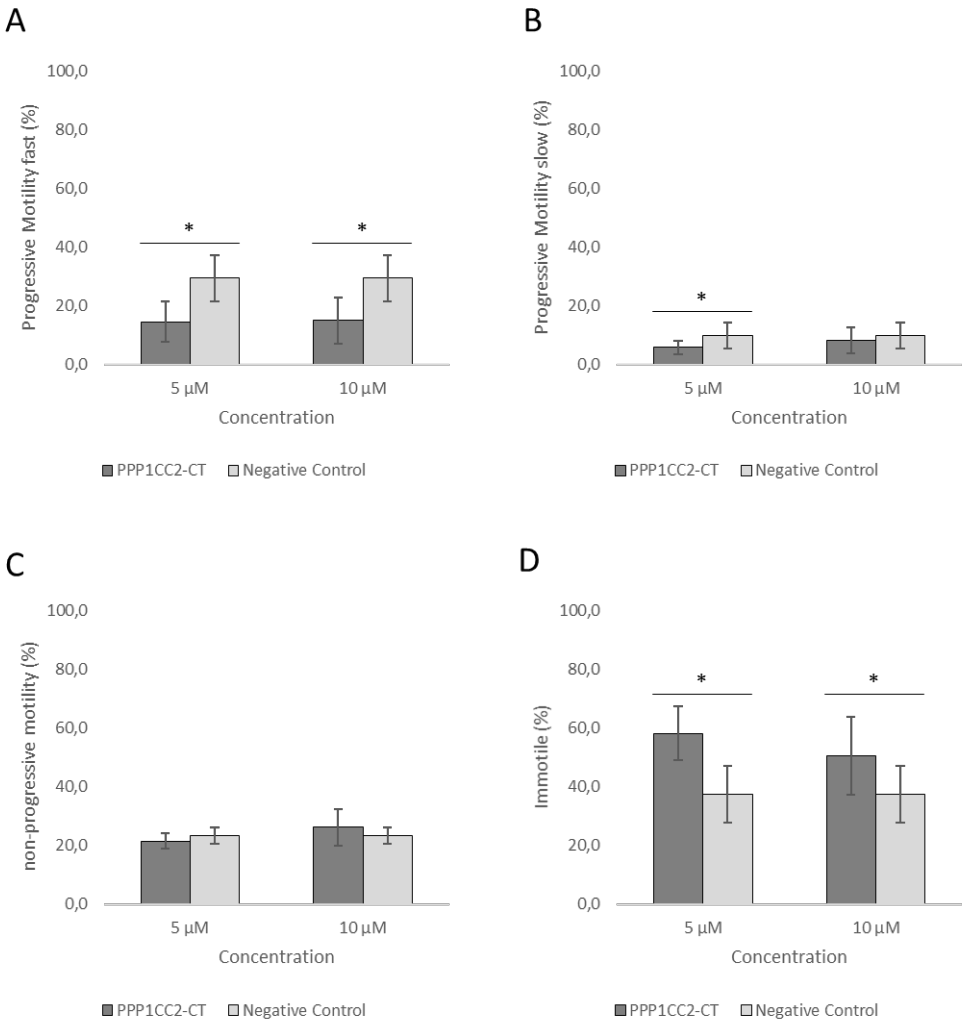

Figure 9 - Impact of the treatment with PPP1CC2-CT peptide in bovine spermatozoa motility parameters: (A) fast progressive motility; (B) slow progressive motility; (C) non-progressive motility; (D) immotile spermatozoa. Graph bars represent the mean values of three independent experiments performed in triplicate. Error bars 95% CI. Statistically significant findings are indicated with a (*). *P<0,05.

3.2.2. AKAP4-BM peptide

Exposure of bovine spermatozoa to 5 μM of AKAP4-BM peptide results in a decrease in fast progressive motility (from 29,5±7,8% in the negative control to 10,0±7,7%). Incubation with 10 μM also induced a decrease in fast progressive motility (from 29,5±7,8% in the negative control to 7,7,0±5,7% in the treatment) and additionally, a decrease in slow progressive motility (from 9,9±4,4% in the negative control to 8,8±3,7% in the treatment). In contrast, immotile spermatozoa increased with both 5 μM (from 37,3±9,6% in the negative control to 56,1±8,3% in the treatment) and 10 μM (from 37,3±9,6% in the negative control to 62,0±13,1% in the treatment) AKAP-BM. Application of the mutated AKAP4-BM peptide did not lead to significant alterations in motility parameters (compared with negative control), except for fast progressive motility, that significantly decrease when spermatozoa were treated with 5μM of AKAP4-BM M (from 29,5±7,8% to 21,5±7,1%) (Figure 10).

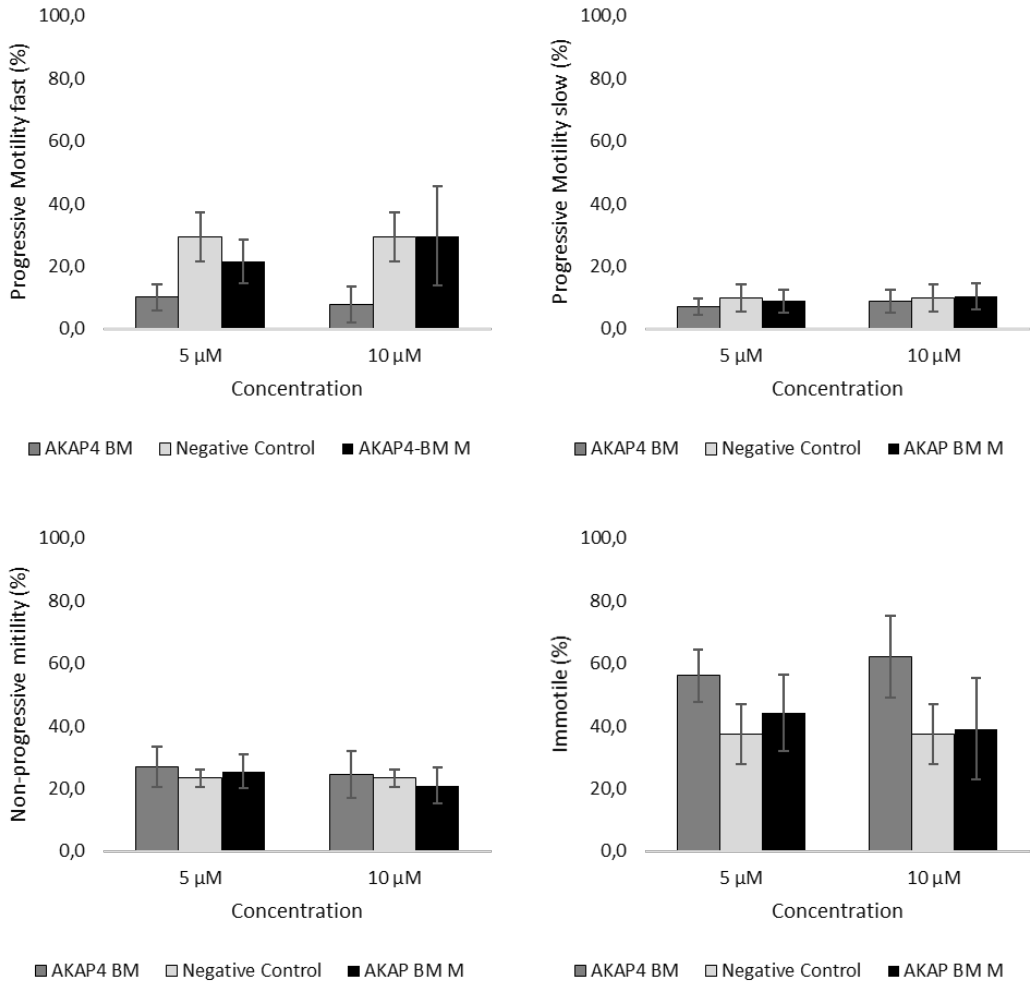

Figure 10 - Impact of the treatment with AKAP4-BM peptide in bovine spermatozoa motility parameters: (A) fast progressive motility; (B) slow progressive motility; (C) non-progressive motility; (D) immotile spermatozoa. Graph bars represent the mean values of three independent experiments performed in triplicate. Error bars 95% CI. Statistically significant findings are indicated with a (*). *P<0,05.

3.3. AKAP4-BM peptide disruptive potential on the AKAP4-PPP1CC2 interaction

3.3.1. PPP1CC2 and AKAP4 interact in spermatozoa

To demonstrate the interaction of PPP1CC2 and AKAP4 in human spermatozoa we performed a co-immunoprecipitation using and isoform-specific anti-PPP1CC2 antibody from normozoospermic human ejaculated sperm samples followed by immunoblotting. Endogenous PPP1CC2 was showed to co-immunoprecipitate with endogenous AKAP4 in normozoospermic human spermatozoa by Western blot (Figure 11, lane 1), as previously reported [148]. However, the signal was weak. This was expected since AKAP4 is present in the insoluble fraction of the spermatozoa and is very resistant to extraction.

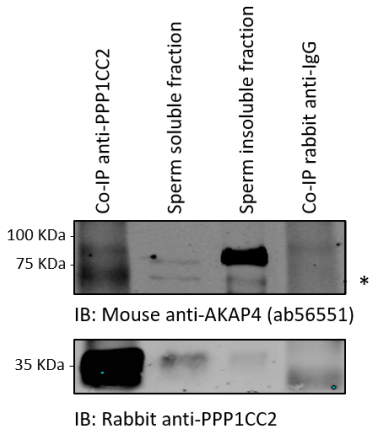

Figure 11 – PPP1CC2 and AKAP4 interact in human spermatozoa revealed by co-immunoprecipitation, using an isoform-specific anti-PPP1CC2 antibody. Human sperm soluble extracts were co-immunoprecipitated with anti-PPP1CC2 antibody and immunoblotted with mouse anti-AKAP4 antibody. Sperm soluble and insoluble extracts corresponding to 4 x 10^6 cells were also loaded. Co-IP, co-immunoprecipitation; IB, immunoblot. Note that mouse anti-AKAP4 antibody has a reported unspecific band (*).

3.3.2. AKAP4-BM peptide disrupts PPP1CC2 and AKAP4 interaction

PPP1CC2 inhibition is required for sperm motility and it is thought that AKAP4 is required for that inhibition. To determine if the effect of the AKAP4-BM peptide in sperm motility is due to AKAP4-PPP1CC2 interaction interference, we perform competition assays in bovine and human spermatozoa using 50μM and 10μM of the peptide. The AKAP4-BM peptide mimics the interaction interface between PPP1CC2 and AKAP4 based on the RVxF motif, one of the best known PPP1C binding motifs. After incubation with the peptides a co-immunoprecipitation of PPP1CC2 was performed and the extracts were run in a 10% SDS-PAGE gel. The results revealed no

differences in the amount of AKAP4 bounded to PPP1CC2 in samples treated with the competition peptide (Figure 12).

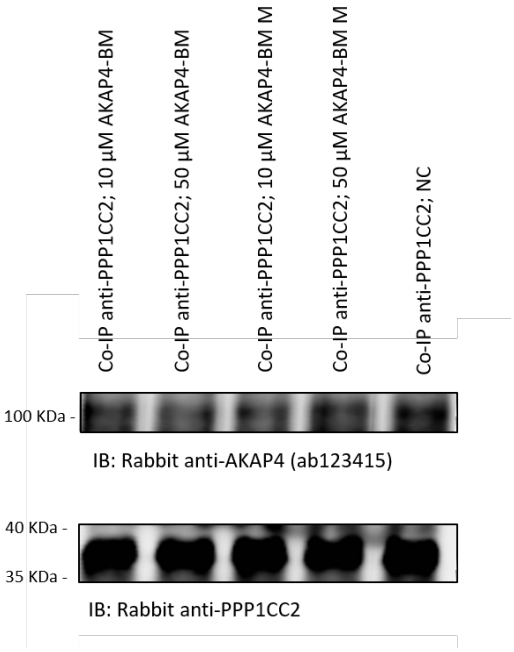

Figure 12 – Competition assay using 10µM and 50µM of AKAP4-BM peptide in human spermatozoa. Human sperm soluble extracts were co-immunoprecipitated with anti-PPP1CC2 antibody and immunoblotted with rabbit anti-AKAP4 antibody. No differences in the amount of AKAP4 bounded to PPP1CC2 were observed in the samples treated with the competition peptides when compared with negative control and with mutated AKAP4-BM peptide.

Due to these results and to further explore this interaction interference, the levels of PPP1CC2 that interact with AKAP4 in HeLa cells transfected with pCMV6-AC-GFP-AKAP4 in the presence of the peptides were determined by blot overlay (Figure 13). All the membranes were overlaid with PPP1CC2 purified protein and the corresponding peptide (AKAP4-BM or AKAP4-BM M) or inhibitor (I2). The control corresponds to the membrane overlaid only with PPP1CC2 purified protein, to establish the amount of PPP1CC2 that normally binds to AKAP4 (Figure 13, C). The results showed that in Hela cells extracts overlaid with AKAP4-BM peptide the amount of PPP1CC2 that binds to endogenous AKAP4 is lower (Figure 13, A), compared with control and with AKAP4-BM M peptide (Figure 13, B). These results suggest that AKAP4-BM peptide binds to PPP1CC2 purified protein, decreasing the amount of PPP1CC2 available for the interaction with endogenous AKAP4. The levels of PPP1CC2 protein bounded to AKAP4 were very similar between membranes overlaid with AKAP4-BM peptide and with I2 (Figure 13, D), an inhibitor of PPP1CC2, as expected. Ponceau S. was used as loading control (Supplementary Figure 1).

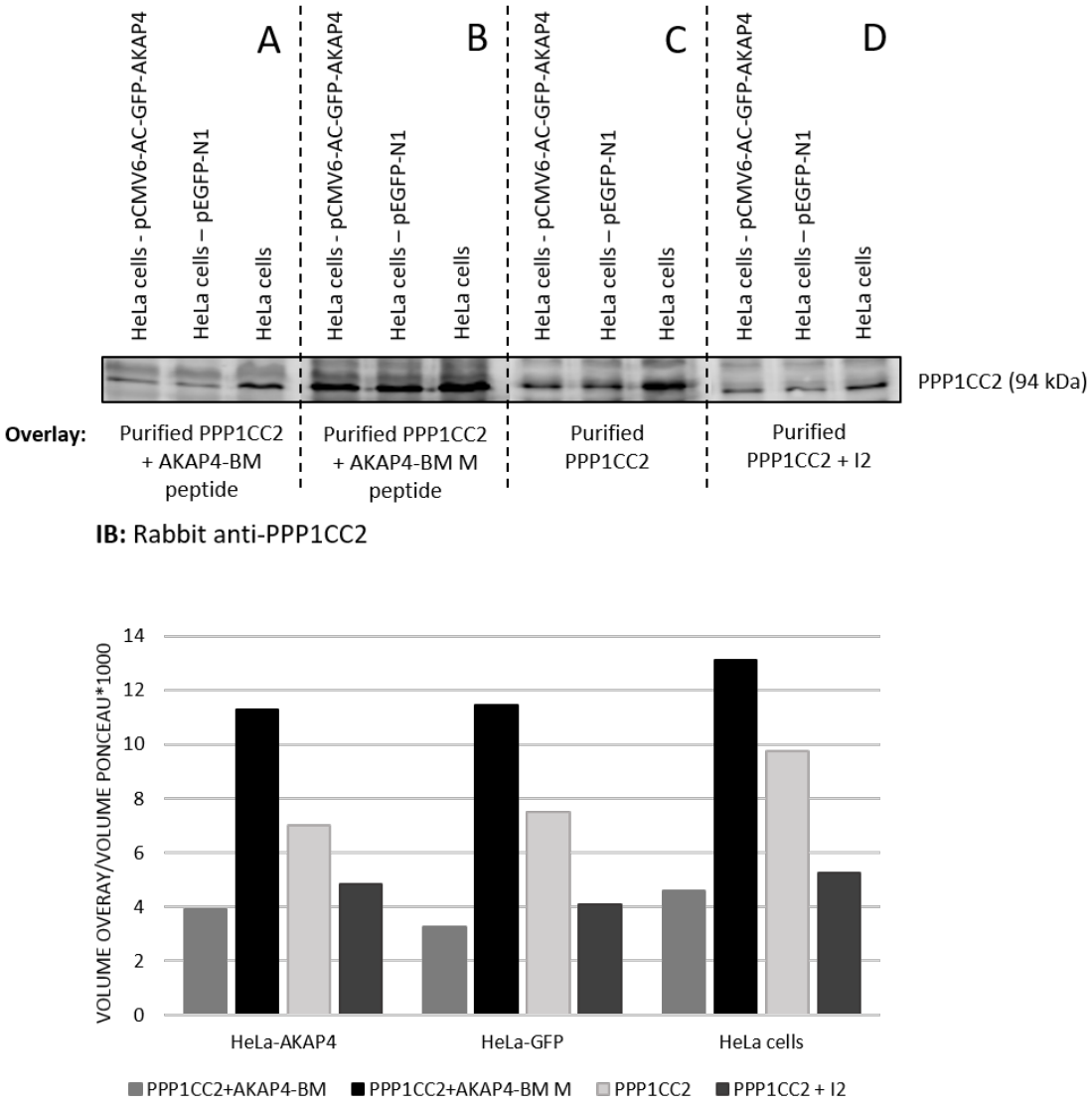

Figure 13 - Disruption of PPP1CC2/AKAP4 interaction by AKAP4-BM peptide. HeLa cells extracts were run on SDS-PAGE gels. Prior to immunoblot with anti-PPP1CC2 antibody the membrane was overlaid with (A) purified PPP1CC2 and AKAP4-BM peptide; (B) purified PPP1CC2 and AKAP4-BM M peptide; (C) purified PPP1CC2 and (D) purified PPP1CC2 and I2. Pixel intensity was quantified using Quantity One ® software and Ponceau S. staining was used as loading control (Supplementary Figure 1). The amount of PPP1CC2 that binds to AKAP4 in the presence of the AKAP4-BM peptide is reduced when compared with AKAP4-BM M peptide and with negative control (PPP1CC2 only).

3.4. Characterization of the PPP1CC2-CT peptide interactome: Identification of proteins that specifically interact with the 22-amino acid C-terminus of the human PPP1CC2

To identify PPP1CC2-specific interactors, human spermatozoa were incubated with biotinylated PPP1CC2-CT peptide for 15 min and a co-immunoprecipitation of the peptide was performed followed by intensity-based label-free quantitative (LFQ) LC-MS/MS analysis. Peptide-spectrum matches and protein identifications were filtered using a "target-decoy approach", a powerful strategy to deliver false positive estimations that can be applied to nearly any MS/MS workflow [149,150], at a false discovery rate (FDR) of 1%, providing confident identification of proteins (FDR < 1%). Two peptides that matched with PPP1CC2-CT peptide were identified (Table 4) and PPP1CC is ranked as 27th most abundant protein which indicates good bait recovery after pull down.

Table 4- PPP1CC2-CT peptides identified by mass spectrometry after co-immunoprecipitation of biotinylated PPP1CC2-CT in human spermatozoa samples.

Sequence	Protein	Start position	End position	Score
KPNATRPVTPPR	P36873	303	314	99,5
PNATRPVTPPR	P36873	304	314	45,829

Mass spectrometry data also showed 73 proteins upregulated in samples incubated with the peptide when compared with the negative controls. Interactors were identified using a student's t-test comparing the LFQ intensities of all proteins identified in replicates of CT with the LFQ intensities of all proteins identified in the control. Proteins were classified as interactors according to their position in the volcano plot (Figure 14). When $\log_2$(CT/NC) and -log(p-value) were plotted against each other in a volcano plot the unspecific background binders appears around zero. The interactors appear on the right side of the volcano plot and the higher the difference between the group means and the p value the more the interactors move to the top right corner of the plot, which is the area of highest confidence for a true interaction. Among these 73 proteins, 23 proteins were classified as contaminants and consequently excluded (e.g. 22 ribosomal proteins and one extracellular matrix glycoprotein). In fact, most ribosomal proteins were also detected in the negative control samples and previous findings indicate that these proteins have high affinity to the magnetic beads [151]. Only proteins that were quantified in at least 3 replicates of one of both conditions were considered.

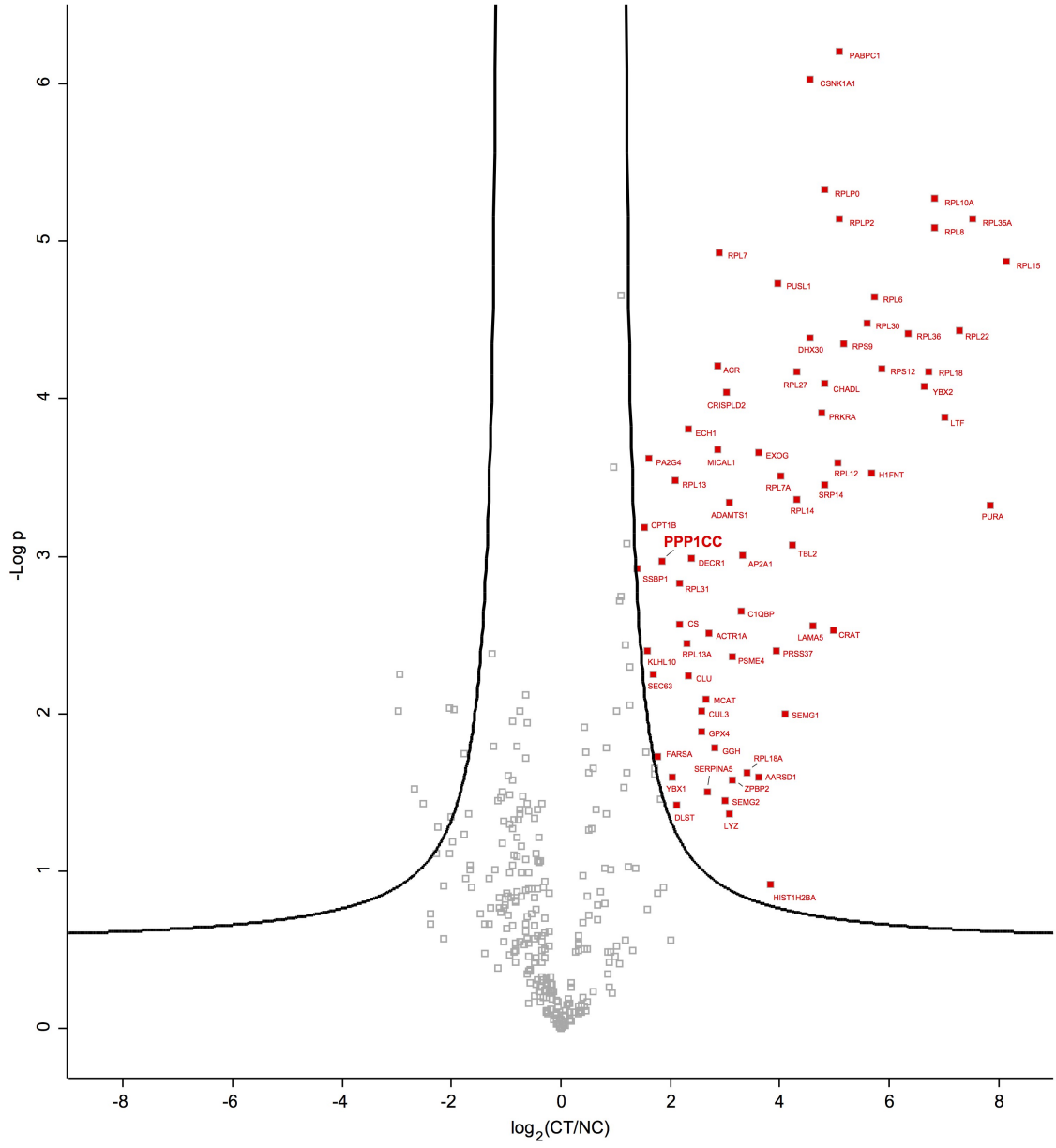

Figure 14 - Identification of PPP1CC2-CT interactors. Proteins are classified as interactors according to their position in the volcano plot. The enriched interactors appear on the right side of the plot, in red.

Thus, we identified 50 proteins that interact with the 22 amino acids C-terminus of human PPP1CC2 (Supplementary Table 9). From those, ten are testis specific/enriched proteins (YBX2, H1FNT, CSNK1A1L, TBL2, PRSS37, HIST1H2BA, ZPBP2, ACR, SERPINA5 and KLHL10). The majority of the proteins identified as PPP1CC2-CT interactors are localized intracellularly (80%) or are secreted (36%). A minority is associated to the membrane (10%) (Table 5).

Analysis of human testicular, epididymal and sperm proteomes allowed the classification of (i) YBX2 as sperm-located epididymal protein also detected in the

sperm-milieu; (ii) TBL2, GPX4 and KLHL10 as sperm-milieu epididymal proteins; (iii) AARSD1 and ECH1 as testicular protein; (iv) H1FNT and CRISPLD2 as a sperm-located testicular protein also detected in sperm milieu; and (v) CLU as a sperm located testicular/epididymal protein also detected in sperm milieu (Table 5). According to the information collected in the Disease and DisGeNET databases, eleven proteins (YBX2, H1FNT, SEMG1, PRSS37, HIST1H2BA, PSME4, SEMG2, ACR, GPX4, PPP1CC and KLHL10) are associated with male infertility phenotypes, more specifically with azoospermia (YBX2, PPP1CC, PA2G4 and KLHL10), oligozoospermia (YBX2, PPP1CC and KLHL10), asthenozoospermia (KLHL10), abnormal spermatogenesis (YBX2) and varicocele (SEMG2). Besides that, twelve PPP1CC2-CT putative interactors are connected to reproductive phenotypes in gene knockout models (YBX2, H1FNT, SEMG1, PRSS37, ZPBP2, PSME4, ACR, SERPINA5, GPX4, YBX3, PPP1CC and KLHL10).

Table 5 – Characterization of the 50 PPP1CC2-CT peptide interactors identified by LC-MS/MS analysis. Loc, localization; I, intracellular; S, secreted; M, membrane.

Uniprot ID	Protein name	Gene name	Tissue expression	Loc	Molecular Function	Human proteomes [152]	Identified in spermatozoa under specific conditions
Q00577	Transcriptional activator protein Pur-alpha	PURA	Mixed	I	Activator, DNA-binding		
P02788	Lactotransferrin	LTF	Tissue enhanced (bone marrow, cervix, uterine)	I, S	Antibiotic, Antimicrobial, DNA-binding, Heparin-binding, Hydrolase, Protease, Serine protease		Decrease ROS level (down; up) [153]; Diabetes type I and II (up) [154]; DNA fragmentation (up) [155]; Obesity (up) [154]; Poor blastocyst development (down) [156]
Q9Y2T7	Y-box-binding protein 2	YBX2	Tissue enriched (testis)	I	DNA-binding, RNA-binding	Sperm-located epididymal protein also detected in sperm-milieu	
Q75WM6	Testis-specific H1 histone	H1FNT	Tissue enriched (testis)	I	Developmental protein, DNA-binding	Sperm-located testicular protein also detected in sperm-milieu	Non-progressive motility (up)[157];
P11940	Polyadenylate-binding protein 1	PABPC1	Expressed in all	I	RNA-binding		
P43155	Carnitine O-acetyltransferase	CRAT	Expressed in all	I	Acyltransferase, Transferase		Poor blastocyst development (down) [156]
P37108	Signal recognition particle 14 kDa protein	SRP14	Expressed in all	I; S	Ribonucleoprotein, RNA-binding		
Q6NUI6	Chondroadherin-like protein	CHADL	Tissue enhanced (cerebral cortex)	I; S			
O75569	Interferon-inducible double-stranded RNA-dependent protein kinase activator A	PRKRA	Expressed in all	I	RNA-binding		
P48729	Casein kinase I isoform alpha	CSNK1A1	Expressed in all	I; M	Kinase, Serine/threonine-protein kinase, Transferase		
Q8N752	Casein kinase I isoform alpha-like	CSNK1A1L	Tissue enriched (testis)	I	Kinase, Serine/threonine-protein kinase, Transferase		
Q7L2E3	Putative ATP-dependent RNA helicase	DHX30	Expressed in all	I; S	Helicase, Hydrolase,		

Uniprot ID	Protein name	Gene name	Tissue expression	Loc	Molecular Function	Human proteomes [152]	Identified in spermatozoa under specific conditions
	DHX30				RNA-binding		
Q9Y4P3	Transducin beta-like protein 2	TBL2	Tissue enriched (testis)	I; S		Sperm-milieu epididymal protein	
P04279	Semenogelin-1	SEMG1	Tissue enriched (seminal vesicle)	S			Decrease ROS level (up; down) [153]; Diabetes type I (up [154]; down [158]); Diabetes type II (up; down) [154]; DNA fragmentation (up) [155]; Idiopathic Infertility (up) [159,160]; IVF failure (up) [159]; Obesity (up) [154];
Q8N0Z8	tRNA pseudouridine synthase-like 1	PUSL1	Expressed in all	I	Isomerase		
A4D1T9	Probable inactive serine protease 37	PRSS37	Tissue enriched (testis)	S			
Q96A08	Histone H2B type 1-A	HIST1H2BA	Tissue enriched (testis)	I	DNA-binding		IVF failure (up) [159]
Q9BTE6	Alanyl-tRNA editing protein Aarsd1	AARSD1	Expressed in all	I		Testicular protein	
Q9Y2C4	Nuclease EXOG, mitochondrial	EXOG	Mixed	I; S	Endonuclease, Hydrolase, Nuclease		
O95782	AP-2 complex subunit alpha-1	AP2A1	Expressed in all	I			
O94973	AP-2 complex subunit alpha-2	AP2A2	Mixed	I			
Q07021	Complement component 1 Q subcomponent-binding protein, mitochondrial	C1QBP	Expressed in all	I			
Q6X784	Zona pellucida-binding protein 2	ZPBP2	Tissue enriched (testis)	S			DNA fragmentation (up) [155]
Q14997	Proteasome activator complex subunit 4	PSME4	Expressed in all	I	Developmental protein		Non-progressive motility (up) [157]
Q9UHI8	A disintegrin and metalloproteinase with thrombospondin motifs 1	ADAMTS1	Tissue enhanced (ovary)	I; M; S	Heparin-binding, Hydrolase, Metallo protease, Protease		
P61626	Lysozyme C	LYZ	Expressed in all	S	Antimicrobial, Bacteriolytic enzyme, Glycosidase, Hydrolase		
Q9H0B8	Cysteine-rich secretory protein LCCL	CRISPLD2	Expressed in all	I; S		Sperm-located	

Uniprot ID	Protein name	Gene name	Tissue expression	Loc	Molecular Function	Human proteomes [152]	Identified in spermatozoa under specific conditions
	domain-containing 2					testicular protein also detected in sperm-milieu	
Q02383	Semenogelin-2	SEMG2	Tissue enriched (seminal vesicle)	S			Decrease ROS level (down)[153]; Idiopathic Infertility (up) [160]; Obesity (down) [158]
P10323	Acrosin	ACR	Tissue enriched (testis)	S	Hydrolase, Protease, Serine protease		DNA fragmentation (up) [155]; Idiopathic Infertility (down) [159]
Q8TDZ2	Protein-methionine sulfoxide oxidase MICAL1	MICAL1	Mixed	I	Actin-binding, Monooxygenase, Oxidored uctase		
Q92820	Gamma-glutamyl hydrolase	GGH	Tissue enhanced (kidney)	S	Hydrolase		Diabetes type I and II (down) [154]; Non-progressive motility (down) [157]
P61163	Alpha-centractin	ACTR1A	Expressed in all	I			
P05154	Plasma serine protease inhibitor	SERPINA5	Tissue enhanced (testis, adrenal gland, liver)	S	Heparin-binding, Protease inhibitor, Serine protease inhibitor		
Q8IVS2	Malonyl-CoA-acyl carrier protein transacylase, mitochondrial	MCAT	Expressed in all	I	Transferase		
Q13618	Cullin-3	CUL3	Expressed in all	I			
P36969	Phospholipid hydroperoxide glutathione peroxidase, mitochondrial	GPX4	Expressed in all	I; S	Developmental protein, Oxidoreductase, Peroxidase	Sperm-milieu epididymal protein	Asthenozoospermia (up)[161]; Idiopathic Infertility (down) [160];
Q16698	2,4-dienoyl-CoA reductase, mitochondrial	DECR1	Expressed in all	I	Oxidoreductase		
Q13011	Delta(3,5)-Delta(2,4)-dienoyl-CoA isomerase, mitochondrial	ECH1	Expressed in all	I	Isomerase	Testicular protein	
P10909	Clusterin	CLU	Expressed in all	I; S	Chaperone	Sperm-located testicular/epididymal protein also detected in sperm-milieu	Diabetes type I and II (up) [154]; DNA fragmentation (up) [155]; Increased age (up) [162]; IVF failure (up) [159]; Idiopathic Infertility (up) [160]; Obesity (up)

Uniprot ID	Protein name	Gene name	Tissue expression	Loc	Molecular Function	Human proteomes [152]	Identified in spermatozoa under specific conditions
							[154]; Poor blastocyst development (up) [156]; Round-headed spermatozoa (up) [163];
O75390	Citrate synthase, mitochondrial	CS	Expressed in all	I; M	Transferase		DNA fragmentation (up) [155]
P36957	Dihydrolipoyllysine-residue succinyltransferase component of 2-oxoglutarate dehydrogenase complex, mitochondrial	DLST	Expressed in all	I	Acyltransferase, Transferase		Asthenozoospermia (down) [157]
P67809	Nuclease-sensitive element-binding protein 1	YBX1	Expressed in all	I	Activator, DNA-binding, Mitogen, Repressor, RNA-binding, DNA-binding, Repressor		
P16989	Y-box-binding protein 3	YBX3	Expressed in all	I	Activator, DNA-binding, Mitogen, Repressor, RNA-binding, DNA-binding, Repressor		
P36873	Serine/threonine-protein phosphatase PP1-gamma catalytic subunit	PPP1CC	Expressed in all	I	Hydrolase, Protein phosphatase		
Q9Y285	Phenylalanine--tRNA ligase alpha subunit	FARSA	Expressed in all	I	Aminoacyl-tRNA synthetase, Ligase		
Q9UGP8	Translocation protein SEC63 homolog	SEC63	Expressed in all	M	Chaperone		
Q9UQ80	Proliferation-associated protein 2G4	PA2G4	Expressed in all	I	Repressor, Ribonucleoprotein, RNA-binding		
Q6JEL2	Kelch-like protein 10	KLHL10	Tissue enriched (testis)	I		Sperm-milieu epididymal protein	
Q92523	Carnitine O-palmitoyltransferase 1, muscle isoform	CPT1B	Expressed in all	M	Acyltransferase, Transferase		
Q04837	Single-stranded DNA-binding protein, mitochondrial	SSBP1	Expressed in all	I	DNA-binding		Non-progressive motility (up) [157]

To confirm the interaction between the PPP1CC2-CT peptide and a protein identified in the LC-MS/MS analysis, a fraction of the co-immunoprecipitation with the biotinylated PPP1CC2-CT peptide was run on a SDS-PAGE gel and immunoblotted with rabbit anti-GPX4 antibody. The results showed that PPP1CC2-CT co-immunoprecipitates with endogenous GPX4 in normozoospermic human spermatozoa (Figure 15, lane 1).

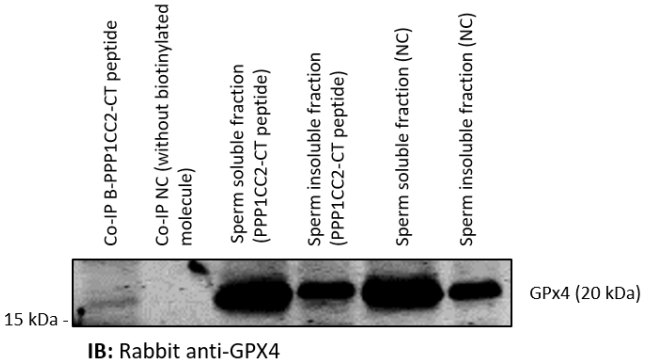

Figure 15 - GPX4 interacts with C-terminus of PPP1CC2 protein. Co-immunoprecipitation of PPP1CC2-CT from ejaculated normozoospermic human sperm sample followed by immunoblot with ant-GPX4 antibody showed PPP1CC2-CT/GPX4 interaction. Sperm soluble and insoluble extracts were also loaded. Co-IP, co-immunoprecipitation; IB, immunoblot.

4. Discussion

In the past decades, PPIs have emerged as promising drug targets. Several approaches were used to modulate these interactions, one of them involves the use of CPPs as intracellular delivery vectors. This short peptide sequences, usually with less than 30 amino acids in length often with positive charge, are able to cross through the cellular membrane and deliver different types of cargo [96,102]. This strategy allows the delivery of drugs that are usually unable to cross an intact lipid barrier. In terms of clinical applications, CPPs can be used to deliver a wide range of therapeutic moieties, including small molecules, liposomes, nanoparticles and biopharmaceuticals including oligonucleotides, peptides and proteins [94,97]. The CPP used in this study to deliver the peptides sequences was penetratin, an inert CPP that efficiently translocate into spermatozoa flagellum [138]. The intracellular accumulation of the TAMRA-labeled peptides was quantified in bovine spermatozoa. AKAP4-BM and PPP1CC2-CT peptides internalized more efficiently than AKAP4-BM M in bovine spermatozoa (Figure 7, A). Those results were in accordance with the preliminary data obtained by fluorescent microscopy and quantitative translocation analyses of the same TAMRA-labeled peptide at 1h in bovine spermatozoa [164]. Jones at al. previously demonstrate that CPPs enter very fast in the mammalian spermatozoa, with a half-time between 1 and 3 min, dependent on the CPP [138]. This study showed that only a few minutes were necessary to the peptides enter the sperm cell, indicate that CPP readily translocate into bovine spermatozoa. Higher concentrations reflect a higher cellular uptake but lower concentrations should be tested to achieve approximately the same intracellular uptake of the peptides. Plasma membrane integrity of spermatozoa could be affected by storage in liquid nitrogen [147,165], increasing the permeability of sperm cells which can affect the uptake results. Further studies using fresh bovine samples and performing a vitality analysis prior to the uptake test are necessary to confirm the results.

Exposure of bovine and human spermatozoa to the competition peptides for 1h and 2h induced significant alterations in motility parameters, without altering cell viability [164]. The present results showed that exposure of bovine spermatozoa to the PPI disruptor peptide sequences induced significant alteration in motility parameters as early as 15 min (Figure 9 and Figure 10).

This study demonstrated that AKAP4-BM, a synthetic peptide that contains a variant of the RVxF motif, was successfully delivered to spermatozoa and led to a significantly

alteration in sperm motility parameters. Upon treatment of bovine spermatozoa with the AKAP4-BM peptide, the percentage of fast progressive motility declined (Figure 10, A). Slow progressive motility also decreased upon exposure to 5 μM of AKAP4-BM peptide, when compared with negative control, and upon exposure to 10 μM of AKAP4-BM peptide, when compared with the treatment with mutated AKAP4-BM peptide. In turn, the percentage of immotile spermatozoa increased significantly (Figure 10, D). Exposure to the mutated AKAP4-BM peptide did not lead to significant differences in motility parameters, when compared to negative control, except for 5 μM of AKAP4-BM M that induced significant decrease in fast progressive motility. Several findings suggest that AKAP/PRKA/PPP1 complex is essential for sperm motility regulation. AKAP4, the major protein of the fibrous sheath of the flagellum, is one of the three AKAPs that have been related to PPP1CC2 [85]. The targeted disruption of the *Akap4* gene in mice compromise sperm flagellum morphology through the lack of fibrous sheath of the principal piece, resulting in male infertility. [21]. In addition, *Akap4* gene knockout in mice change PPP1CC2 activity and phosphorylation, as demonstrated by Huang and colleagues [89]. Recently, Silva et al. (2017) [148] reported for the first time that AKAP4 interacts with PPP1CC2 in ejaculated human spermatozoa, which was also confirmed in this study. Since PPP1CC2 inhibition is required for sperm motility and AKAP4 seems to be involved in that inhibition, we hypothesized that the loss of sperm motility resulting from the AKAP4-BM peptide treatment was due to PPP1CC2-AKAP4 interaction disruption. To test that hypothesis, competition assays using different concentrations of the AKAP4-BM peptide were performed *in vitro*. The results demonstrated that upon exposure to the competition peptide, the amount of PPP1CC2 that binds to AKAP4 was reduced, which support the theory that the peptide interfere with PPP1CC2-AKAP4 interaction (Figure 13).

Further studies are needed to determine the alteration on PPP1CC2 activity and phosphorylation status, upon exposure to the AKAP4-BM peptide, by using phosphatase assays and of global protein serine/threonine phosphorylation status. The assessment of PPP1CC2 activity and global phosphorylation levels might help to understand the impact of peptides at the cellular level that possibly affect the spermatozoa motility. The same experiments should be performed in human spermatozoa to confirm and clarify the impact of peptides in spermatozoa.

Upon treatment with the PPP1CC2-CT peptide the percentage of fast progressive motility significantly decreased with both concentrations tested (Figure 9, A) and the percentage of immotile spermatozoa significantly increased (Figure 9, D), similarly to what was already showed for 10 μM and 20 μM of the same peptide at 1h and 2h

[164]. Regarding slow progressive motility, significant alterations were only observed upon treatment with 5 μM of PPP1CC2 peptide. The effect observed in sperm motility seems to be independent of peptide concentration, as previously demonstrated. These results were in accordance with what was described for these peptides, showing that peptides rapidly entry in the sperm cells and induced significant alterations in sperm motility as early as 15 min of incubation. The same experiments should be performed in human spermatozoa to confirm and clarify the impact of peptides in spermatozoa. Further studies are necessary to investigate if the impact of the peptides in sperm motility is reversible, when the peptide is removed.

PPP1CC2-CT peptide mimics the unique 22 amino acid C-terminus of PPP1CC2 and probably compete with isoform-specific interactors of this phosphatase, affecting its action and, thus, sperm motility (Figure 16, A). Endophilin B1t, a testis enriched isoform of the somatic endophilin B1a, and the spermatogenic zip protein (Spz1) [67,68] are two isoform-specific interactors previously identified in testes. In order to identify other PPP1CC2-specific interactors, the interactome of PPP1CC2-CT peptide was performed in human spermatozoa. Of the 50 PPP1CC2-CT interactors identified by LC-MS/MS analysis, 10 were identified as testes specific/enriched proteins. Eight proteins were associated with abnormal sperm motility phenotypes (H1FNT, SEMG-1, PSME4, GGH, SERPINA5, mGPx4, DLST and SSBP1).

One of the interactors identified was GPx4 – identified for the first time in pig liver [166] and involved in several biological functions, including sperm maturation [167,168]. Despite their expression in most mammalian tissues, larger amounts are present in testes [169] and spermatozoa. In sperm cells two isoforms were described – sperm nucelar GPx4 (snGPx4) and midpiece GPx4 (mGPx4). In mature spermatozoa, mGPx4 exists as an enzymatically inactive insoluble protein, constituting 50 percent of the capsule material that surround the mitochondrial sheath where is cross-linked with other capsule proteins [167]. Thus, mGPx4 constitute the major structural constituent of mitochondrial capsules that surround mitochondria in the midpiece of mature spermatozoa. GPX4 was identified in asthenozoospermic male [161] and GPx4 gene knockout mice was infertile due to abnormal sperm motility, morphology and physiology [168,170,171]. The infertility phenotype observed in mice lacking GPx4 results from midpiece structural defects and not from loss of enzymatic activity [170,171]. In the present study was showed by LC-MS/MS and by Western Blot that GPx4 interacts with the 22 amino acids C-terminus of PPP1CC2, constituting a putative isoform-specific interactor. Additionally, both PPP1CC2 and GPx4 activity deregulation was previously associated with sperm motility arrest and both proteins are present in sperm midpiece,

supporting the hypothesis that these proteins might have a common role in spermatozoa motility. However, further studies are needed to explore PPP1CC2-GPx4 interaction and clarify the role of this complex on sperm motility.

Disruption of motility-related PPP1CC2-PIP interactions potentially generate active PPP1CC2 that dephosphorylate a subset of substrates and prevent motility acquisition. The identification of novel PPP1CC2-specific interactors represents a good target for new contraceptive methods, capable of modulate PPP1CC2 activity, an isoform only present in testes/spermatozoa, by targeting/disrupting these interactions.

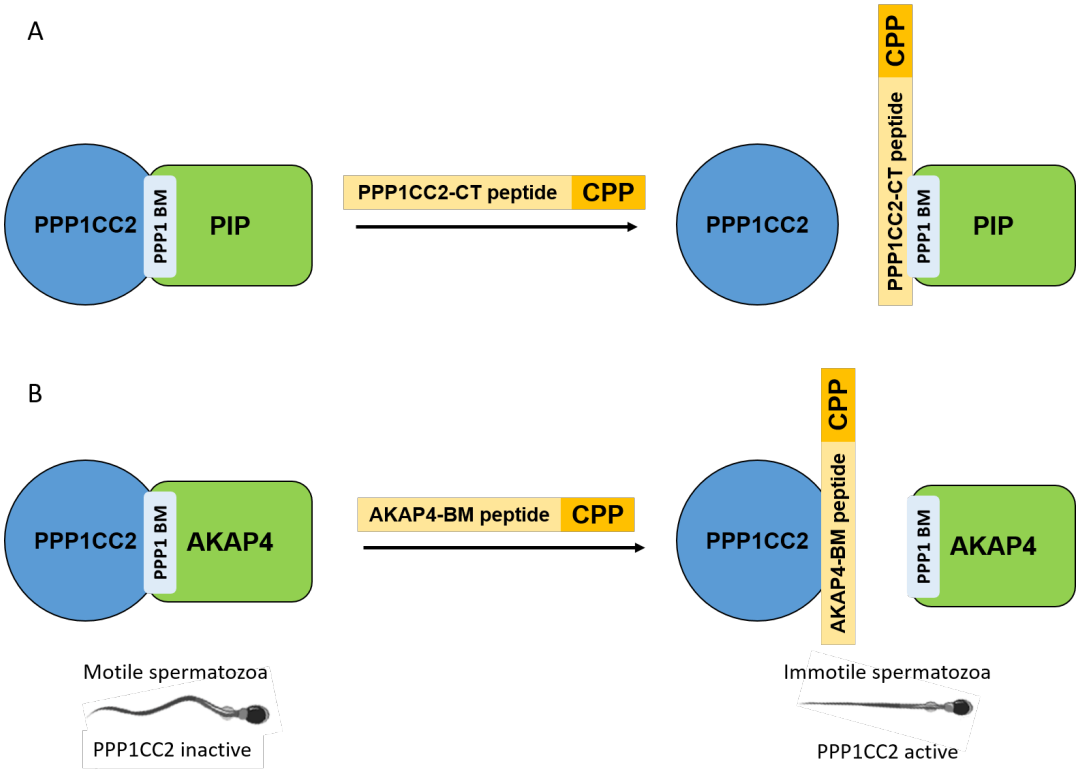

Figure 16 - Disruption of PPP1CC2- specific PIP and PPP1CC2/AKAP4 complex using cell-penetrating peptides as drug intracellular delivery system. (A) In spermatozoa, PPP1CC2 usually interacts with PIP. In the presence of PPP1CC2-CT peptide, PIP that specifically bind to the 22-amino acid C-terminus of PPP1CC2, bind to the peptide instead of bind to endogenous protein, resulting in activation of PPP1CC2 and, thus, arrest of sperm motility. (B) AKAP4-PPP1CC2 complex is essential for regulation of sperm motility. When spermatozoa were treated with AKAP4-BM mutant peptide, the peptide sequence interacts with endogenous PPP1CC2 through the RVxF motif, competing with endogenous AKAP4. The disruption of AKAP4/PPP1CC2 interaction results in active PPP1CC2 and, consequently, immotile spermatozoa. PPP1 BM, PPP1 binding motif.

5. Conclusions and future perspectives

5.1. Conclusions

The main objective of this thesis was to modulate protein complexes and, consequently, sperm motility using cell-penetrating peptides that specifically interact with non-hormonal targets selectively expressed in testis and sperm.

To achieve this goal, PPP1CC2-specific interactions and PPP1CC2/AKAP4 complex were successfully modulated in spermatozoa using lower concentrations and incubation times of CPPs previously synthetized in the laboratory with known impact on sperm motility.

A peptide sequence that mimics the interaction interface between PPP1CC2 and AKAP4 was successfully delivered to the spermatozoa with a significantly impact in sperm motility, as previously showed with higher concentrations and longer incubation times. Competition assays using the competition peptide allowed to confirm that the effect on sperm motility is due to PPP1CC2/AKAP4 interaction interference.

A CPP was used to deliver a peptide sequence that mimics the unique 22 amino acid C-terminus of PPP1CC2 into spermatozoa, compromising isoform-specific interaction and, thus, affecting sperm motility, confirming the previously results obtained with higher concentrations at 1h and 2h of incubation. The same peptide was used to identify isoform-specific interactors, some of them associated with male infertility and abnormal sperm motility. In fact, despite some PPP1CC2-specific interactors were reported in testes, this is the first report of PPP1CC2 C-terminus interactome in spermatozoa. Fifty proteins were identified using LC-MS/MS analysis and one of them – GPx4 – was validated by Western Blot analysis. These proteins can constitute potential targets for new male contraceptives.

Concluding, this work modulated protein complexes involved in spermatozoa motility in human and bovine spermatozoa and identify PPP1CC2 C-terminus-specific interactors that can be used as potential targets for new male contraceptive methods.

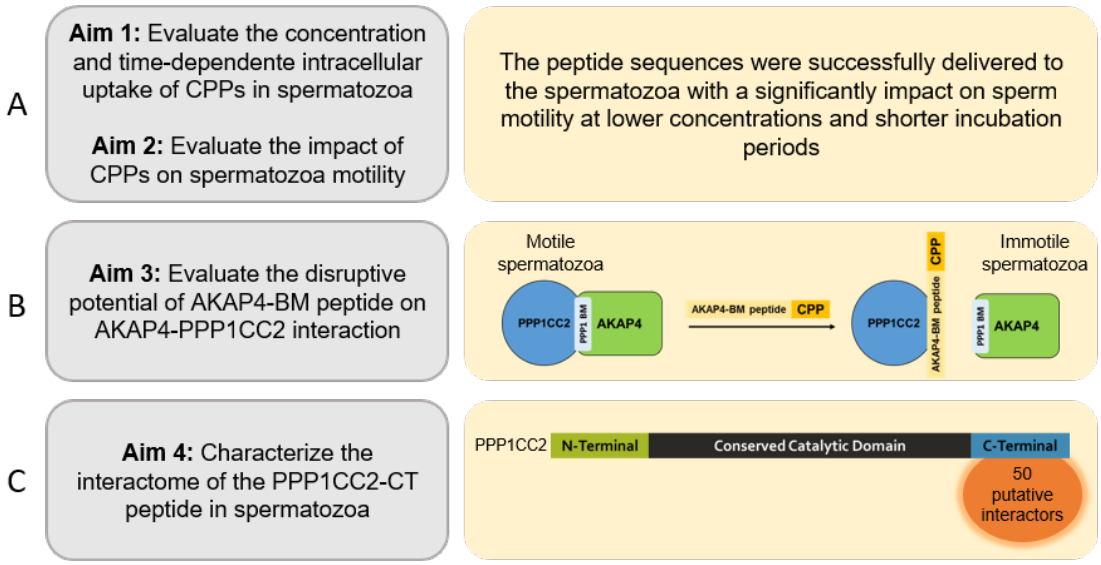

Figure 17 - Overview of the main goals and main conclusions of this thesis. (A) All peptide sequences tested were successfully delivered to the cell, with a significant impact on sperm motility at lower concentration and shorter incubation times than previously observed at our laboratory; (B) The AKAP4-BM peptide was demonstrated to disrupt the PPP1CC2-AKAP4 interaction; (C) Fifty putative interactors of PPP1CC2-CT were identified by LC-MS/MS analysis.

5.2. Future perspectives

This study validated the previous results from the laboratory that designed peptides can efficiently modulate spermatozoa complexes and consequently modulate sperm motility. Future work should focus upon the identification of novel sperm-specific targets and design of peptide sequences conjugated with CPP to modulate them. The most promising candidates will be validated in human sperm samples and detailed *in vivo* studies will be performed. *In vivo* studies should allow, for example, to access the capacity of these compounds to cross the blood-epididymis barrier.

References

1. Keber R, Rozman D, Horvat S. Sterols in Spermatogenesis and Sperm maturation. J Lipid Res. 2012;54(1):20–33.
2. Silva J, Freitas MJ, Fardilha M. Phosphoprotein Phosphatase 1 Complexes in Spermatogenesis. Curr Mol Pharmacol. 2014;7(2).
3. Knobil E, Neill J. The Physiology of Reproduction. 2nd ed. New York: Raven Press; 1994.
4. Kretser DM De, Loveland KL, Meinhardt A, Simorangkir D, Wreford N. Spermatogenesis. Hum Reprod. 1998;13:1–8.
5. Ehmcke J, Wistuba J, Schlatt S. Spermatogonial stem cells: Questions, models and perspectives. Hum Reprod Update. 2006;12(3):275–82.
6. Lianhua D, Maoliang R, Zhi L, Fuzhi P, Bin C. The role of ubiquitin-proteasome pathway in spermatogenesis. Yi chuan = Hered. 2016 Sep;38(9):791–800.
7. Rossitto M, Philibert P, Poulat F. Molecular events and signalling pathways of male germ cell differentiation in mouse. Semin Cell Dev Biol. 2015;45:84–93.
8. Misell LM, Holochwost D, Boban D, Santi N, Shefi S, Hellerstein MK, Turek PJ. A Stable Isotope-Mass Spectrometric Method for Measuring Human Spermatogenesis Kinetics In Vivo. J Urol. 2006;175(1):242–6.
9. Almeida FFL, Leal MC, França LR. Testis morphometry, duration of spermatogenesis, and spermatogenic efficiency in the wild boar (Sus scrofa scrofa). Biol Reprod. 2006;75(5):792–9.
10. Zeng W, Avelar G, Rathi R, Franca L, Dobrinsky I. The Length of the Spermatogenic Cycle Is Conserved in Porcine and Ovine Testis Xenografts. J Androl. 2006;27(4):527–33.
11. Fawcett DW. The anatomy of the mammalian spermatozoon with particular reference to the guinea pig. Zeitschrift für Zellforsch und Mikroskopische Anat. 1965;67(3):279–96.
12. Pesch S, Bergmann M. Structure of mammalian spermatozoa in respect to viability, fertility and cryopreservation. Micron. 2006;37(7):597–612.
13. Brewer L, Corzett M, Balhorn R. Condensation of DNA by spermatid basic nuclear proteins. J Biol Chem. 2002;277(41):38895–900.
14. Dadoune J-P. Expression of mammalian spermatozoal nucleoproteins. Microsc Res Tech. 2003 May;61(1):56–75.
15. Hammoud SS, Nix DA, Zhang H, Purwar J, Carrell DT, Cairns BR. Distinctive chromatin in human sperm packages genes for embryo development. Nature. 2009;460(7254):473–8.
16. Oliva R. Protamines and male infertility. Hum Reprod Update. 2006;12(4):417–35.
17. Ho H-C, Suarez SS. Characterization of the Intracellular Calcium Store at the Base of the Sperm Flagellum That Regulates Hyperactivated Motility1. Biol Reprod. 2003 May;68(5):1590–6.
18. Oko RJ. Developmental expression and possible role of perinuclear theca proteins in mammalian spermatozoa. Reprod Fertil Dev. 1995;7(4):77–797.
19. Moreno RD, Ramalho-Santos J, Sutovsky P, Chan EKL. Vesicular Traffic and Golgi Apparatus Dynamics During Mammalian Spermatogenesis: Implications for Acrosome Architecture. Biol Reprod. 2000;63(1):89–98.
20. Yoshinaga K, Toshimori K. Organization and modifications of sperm acrosomal molecules during spermatogenesis and epididymal maturation. Microsc Res Tech. 2003 May 1;61(1):39–45.
21. Miki K, Willis WD, Brown PR, Goulding EH, Fulcher KD, Eddy EM. Targeted Disruption of the Akap4 Gene Causes Defects in Sperm Flagellum and Motility. Dev Biol. 2002;248(2):331–42.
22. Inaba K. Molecular architecture of the sperm flagella: molecules for motility and signaling. Zoolog Sci. 2003;20(9):1043–56.
23. Brown PR, Miki K, Harper DB, Eddy EM. A-kinase Anchoring Protein 4 Binding Proteins in the Fibrous Sheath of the Sperm Flagellum. Biol Reprod. 2003;68(6):2241–8.
24. Fardilha M, Silva JV, Conde M. Reprodução Humana Masculina - Princípios Fundamentais. 1st ed. Charleston, SC: ARC Publishing; 2015.
25. Turner RM. Moving to the beat: a review of mammalian sperm motility regulation. Reprod Fertil Dev. 2006;18:25–38.
26. Carrera A, Gerton GL, Moss SB. The major fibrous sheath polypeptide of mouse sperm:

structural and functional similarities to the A-kinase anchoring proteins. Dev Biol. 1994;165(1):272–84.
27. Paoli D, Gallo M, Rizzo F, Baldi E, Francavilla S, Lenzi A, Lombardo F, Gandini L. Mitochondrial membrane potential profile and its correlation with increasing sperm motility. Fertil Steril. 2011;95(7):2315–9.
28. Suarez SS, Pacey AA. Sperm transport in the female reproductive tract. Hum Reprod Update. 2006;12(1):23–37.
29. Turner RM. Tales from the tail: what do we really know about sperm motility? J Androl. 2003;24(6):790–803.
30. Vadnais ML, Aghajanian HK, Lin A, Gerton GL. Signaling in sperm: toward a molecular understanding of the acquisition of sperm motility in the mouse epididymis. Biol Reprod. 2013;89(5):127.
31. Sostaric E, Aalberts M, Gadella BM, Stout TAE. The roles of the epididymis and prostasomes in the attainment of fertilizing capacity by stallion sperm. Anim Reprod Sci. 2008;107(3–4):237–48.
32. Baker MA, Hetherington L, Weinberg A, Naumovski N, Velkov T, Pelzing M, Dolman S, Condina MR, Aitken RJ. Analysis of phosphopeptide changes as spermatozoa acquire functional competence in the epididymis demonstrates changes in the post-translational modification of izumo1. J Proteome Res. 2012;11(11):5252–64.
33. Vijayaraghavan S, Stephens DT, Trautman K, Smith GD, Khatra B, da Cruz e Silva EF, Greengard P. Sperm motility development in the epididymis is associated with decreased glycogen synthase kinase-3 and protein phosphatase 1 activity. Biol Reprod. 1996;54:709–18.
34. Huang Z, Vijayaraghavan S. Increased Phosphorylation of a Distinct Subcellular Pool of Protein Phosphatase, PP1gamma2, During Epididymal Sperm Maturation. Biol Reprod. 2004;70(2):439–47.
35. Piomboni P, Focarelli R, Stendardi A, Ferramosca A, Zara V. The role of mitochondria in energy production for human sperm motility. Int J Androl. 2012;35(2):109–24.
36. Katz DF, Yanagimachi R. Movement characteristics of hamster spermatozoa within the oviduct. Biol Reprod. 1980;22(4):759–64.
37. Suarez SS. Control of hyperactivation in sperm. Hum Reprod Update. 2008;14(6):647–57.
38. Suarez SS, Ho HC. Hyperactivated motility in sperm. Reprod Domest Anim. 2003;38(2):119–24.
39. Ho H, Granish KA, Suarez SS. Hyperactivated motility of bull sperm is triggered at the axoneme by Ca2+ and not cAMP. Dev Biol. 2002;250(1):208–17.
40. Morales P, Overstreet JW, Katz DF. Changes in human sperm motion during capacitation in vitro. J Reprod Fertil. 1988;83(1):119–28.
41. Ho HC, Suarez SS. Hyperactivation of mammalian spermatozoa: Function and regulation. Reproduction. 2001;122(4):519–26.
42. Si Y, Okuno M. Role of tyrosine phosphorylation of flagellar proteins in hamster sperm hyperactivation. Biol Reprod. 1999;61(1):240–6.
43. Miki K. Energy metabolism and sperm function. Soc Reprod Fertil Suppl. 2007;65:309–25.
44. du Plessis S, Agarwal A, Mohanty G, van der Linde M. Oxidative phosphorylation versus glycolysis: what fuel do spermatozoa use? Asian J Androl. 2015;17(2):230.
45. Miki K, Qu W, Goulding EH, Willis WD, Bunch DO, Strader LF, Perreault SD, Eddy EM, O ’brien DA. Glyceraldehyde 3-phosphate dehydrogenase-S, a sperm-specific glycolytic enzyme, is required for sperm motility and male fertility. Proc Natl Acad Sci. 2004;101(47):16501–6.
46. Danshina P V, Geyer CB, Dai Q, Goulding EH, Willis WD, Kitto GB, McCarrey JR, Eddy EM, O’Brien DA. Phosphoglycerate kinase 2 (PGK2) is essential for sperm function and male fertility in mice. Biol Reprod. 2010 Jan;82(1):136–45.
47. Cohen PTW. Protein phosphatase 1-targeted in many directions. J Cell Sci. 2002;115(Pt 2):241–56.
48. Barford D, Das AK, Egloff M-P. The Structure and Mechanisms of Protein Phosphatases: Insights into Catalysis and Regulation. Annu Rev Biophys Biomol Struct. 1998 Jun;27(1):133–64.
49. Cohen PTW. Novel protein serine/threonine phosphatases: Variety is the spice of life. Trends Biochem Sci. 1997;22(7):245–51.

50. Wera S, Hemmingst BA. Serine/threonine protein phosphatases. Biochem J. 1995;311:17–29.
51. Fardilha M, Esteves SLC, Korrodi-Gregório L, da Cruz e Silva O a B, da Cruz e Silva FF. The physiological relevance of protein phosphatase 1 and its interacting proteins to health and disease. Curr Med Chem. 2010;17(33):3996–4017.
52. Chakrabarti R, Kline D, Lu J, Orth J, Pilder S, Vijayaraghavan S. Analysis of Ppp1cc-null mice suggests a role for PP1gamma2 in sperm morphogenesis. Biol Reprod. 2007;76:992–1001.
53. Sinha N, Puri P, Nairn AC, Vijayaraghavan S. Selective Ablation of Ppp1cc Gene in Testicular Germ Cells Causes Oligo-Teratozoospermia and Infertility in Mice. Biol Reprod. 2013;89(5):128–128.
54. Fardilha M, Ferreira M, Pelech S, Vieira S, Rebelo S, Korrodi-Gregorio L, Sousa M, Barros A, Silva V, da Cruz e Silva OAB, da Cruz e Silva EF. “Omics” of human sperm: profiling protein phosphatases. OMICS. 2013;17(9):460–72.
55. Varmuza S, Jurisicova A, Okano K, Hudson J, Boekelheide K, Shipp EB. Spermiogenesis is impaired in mice bearing a targeted mutation in the protein phosphatase 1cgamma gene. Dev Biol. 1999;205:98–110.
56. Sinha N, Pilder S, Vijayaraghavan S. Significant Expression Levels of Transgenic PPP1CC2 in Testis and Sperm Are Required to Overcome the Male Infertility Phenotype of Ppp1cc Null Mice. PLoS One. 2012;7(10):1–13.
57. Soler DC, Kadunganattil S, Ramdas S, Myers K, Roca J, Slaughter T, Pilder SH, Vijayaraghavan S. Expression of transgenic PPP1CC2 in the testis of Ppp1cc-null mice rescues spermatid viability and spermiation but does not restore normal sperm tail ultrastructure, sperm motility, or fertility. Biol Reprod. 2009;81(May):343–52.
58. Korrodi-Gregório L, Ferreira M, Vintém AP, Wu W, Muller T, Marcus K, Vijayaraghavan S, Brautigan DL, Odete AB, Fardilha M, Edgar F. Identification and characterization of two distinct PPP1R2 isoforms in human spermatozoa. BMC Cell Biol. 2013;14:2–14.
59. Fardilha M, Esteves SLC, Korrodi-Gregório L, Pelech S, da Cruz e Silva OAB, da Cruz e Silva E. Protein phosphatase 1 complexes modulate sperm motility and present novel targets for male infertility. Mol Hum Reprod. 2011;17(8):466–77.
60. Smith GD, Wolf DP, Trautman KC, da Cruz e Silva EF, Greengard P, Vijayaraghavan S. Primate sperm contain protein phosphatase 1, a biochemical mediator of motility. Biol Reprod. 1996;54:719–27.
61. Si Y. Hyperactivation of hamster sperm motility by temperature-dependent tyrosine phosphorylation of an 80-kDa protein. Biol Reprod. 1999;61(1):247–52.
62. Signorelli JR, Díaz ES, Fara K, Barón L, Morales P. Protein phosphatases decrease their activity during capacitation: A new requirement for this event. PLoS One. 2013;8(12):e81286.
63. Ceulemans H, Bollen M. Functional Diversity of Protein Phosphatase-1, a Cellular Economizer and Reset Button. Physiol Rev. 2004;84(1).
64. Virshup DM, Shenolikar S. From Promiscuity to Precision: Protein Phosphatases Get a Makeover. Mol Cell. 2009;33(5):537–45.
65. Boens S, Szekér K, Van Eynde A, Bollen M. Interactor-guided dephosphorylation by protein phosphatase-1. Methods Mol Biol. 2013;1053:271–81.
66. Heroes E, Lesage B, Görnemann J, Beullens M, Van Meervelt L, Bollen M. The PP1 binding code: A molecular-lego strategy that governs specificity. Vol. 280, FEBS Journal. 2013. p. 584–95.
67. Hrabchak C, Varmuza S. Identification of the spermatogenic zip protein Spz1 as a putative protein phosphatase-1 (PP1) regulatory protein that specifically binds the PP1CC2 splice variant in mouse testis. J Biol Chem. 2004;279(35):37079–86.
68. Hrabchak C, Henderson H, Varmuza S. A Testis Specific Isoform of Endophilin B1 , Endophilin B1t , Interacts Specifically with Protein Phosphatase-1c γ 2 in Mouse Testis and Is Abnormally Expressed in PP1c γ Null Mice. Biochemistry. 2007;46:4635–44.
69. Matsuura M, Yogo K. TMEM225: A possible protein phosphatase 1γ2 (PP1γ2) regulator localizes to the equatorial segment in mouse spermatozoa. Mol Reprod Dev. 2015 Feb;82(2):139–48.
70. Bhattacharjee R, Goswami S, Dudiki T, Popkie AP, Phiel CJ, Kline D, Vijayaraghavan S. Targeted disruption of glycogen synthase kinase 3A (GSK3A) in mice affects sperm motility

resulting in male infertility. Biol Reprod. 2015;92(3):65.
71. Chakrabarti R, Cheng L, Puri P, Soler D, Vijayaraghavan S. Protein phosphatase PP1gamma2 in sperm morphogenesis and epididymal initiation of sperm motility. Asian J Androl. 2007;9(4):445–52.
72. Hui L, Lu J, Pilder SH. The Mouse t Complex Gene Tsga2, Encoding Polypeptides Located in the Sperm Tail and Anterior Acrosome, Maps to a Locus Associated with Sperm Motility and Sperm-Egg Interaction Abnormalities. Biol Reprod. 2006;74(4):633–43.
73. Zhang J, Zhang L, Zhao S, Lee EY. Identification and characterization of the human HCG V gene product as a novel inhibitor of protein phosphatase-1. Biochemistry. 1998;37(47):16728–34.
74. Pilder SH, Olds-Clarke P, Phillips DM, Silver LM. Hybrid sterility-6: a mouse t complex locus controlling sperm flagellar assembly and movement. Vol. 159, Developmental biology. 1993. p. 631–42.
75. Chun Y, Park J, Kim G, Shima H, Nagao M, Kim M, Chung M. A sds22 Homolog That Is Associated with the Testis- Specific Serine / Threonine Protein Phosphatase 1 gamma 2 in Rat Testis. Biochem Biophys Res Commun. 2000;976:972–6.
76. Mishra S, Somanath PR, Huang Z, Vijayaraghavan S. Binding and Inactivation of the Germ Cell-Specific Protein Phosphatase PP1 2 by sds22 During Epididymal Sperm Maturation. Biol Reprod. 2003;69(5):1572–9.
77. Huang Z, Khatra B, Bollen M, Carr DW, Vijayaraghavan S. Sperm PP1 gamma 2 Is Regulated by a Homologue of the Yeast Protein Phosphatase Binding Protein sds22. Biol Reprod. 2002;67(6):1936–42.
78. Cheng L, Pilder S, Nairn AC, Ramdas S, Vijayaraghavan S. PP1CC2 and PPP1R11 are parts of a multimeric complex in developing testicular germ cells in which their steady state levels are reciprocally related. PLoS One. 2009;4(3):14–20.
79. Kwon YG, Lee SY, Choi Y, Greengard P, Nairn AC. Cell cycle-dependent phosphorylation of mammalian protein phosphatase 1 by cdc2 kinase. Proc Natl Acad Sci U S A. 1997;94(6):2168–73.
80. Liu GWY, Wang RH, Dohadwala M, Schönthal AH, Villa-Moruzzi E, Berndt N. Inhibitory phosphorylation of PP1α catalytic subunit during the G1/S transition. J Biol Chem. 1999;274(41):29470–5.
81. Huang Z, Myers K, Khatra B, Vijayaraghavan S. Protein 14-3-3zeta binds to protein phosphatase PP1gamma2 in bovine epididymal spermatozoa. Biol Reprod. 2004;71(1):177–84.
82. Puri P, Acker-Palmer A, Stahler R, Chen Y, Kline D, Vijayaraghavan S. Identification of testis 14-3-3 binding proteins by tandem affinity purification. Spermatogenesis. 2011;1(4):354–65.
83. Burton KA, Treash-osio B, Muller CH, Dunphy EL, Mcknight GS. Deletion of Type II alpha Regulatory Subunit Delocalizes Protein Kinase A in Mouse Sperm without Affecting Motility or Fertilization. J Biol Chem. 1999;274(34):24131–6.
84. Vijayaraghavan S, Goueli SA, Davey MP, Carr DW. Protein Kinase A-anchoring Inhibitor Peptides Arrest Mammalian Sperm Motility. J Biol Chem. 1997;272(8):4747–52.
85. Turner RMO, Musse MP, Mandal A, Klotz K, Friederike C, Jayes L, Herr JC, Gerton GL, Moss SB, Chemes HE. Molecular Genetic Analysis of Two Human Sperm Fibrous Sheath Proteins, AKAP4 and AKAP3, in Men With Dysplasia of the Fibrous Sheath. J Androl. 2001;22(2):302–15.
86. Moretti E, Scapigliati G, Pascarelli NA, Baccetti B, Collodel G. Localization of AKAP4 and tubulin proteins in sperm with reduced motility. Asian J Androl. 2007;9(5):641–9.
87. Reinton N, Collas P, Haugen TB, Skâlhegg BS, Hansson V, Jahnsen T, Taskén K. Localization of a novel human A-kinase-anchoring protein, hAKAP220, during spermatogenesis. Dev Biol. 2000;223(1):194–204.
88. Schillace R V., Voltz JW, Sim ATR, Shenolikar S, Scott JD. Multiple Interactions within the AKAP220 Signaling Complex Contribute to Protein Phosphatase 1 Regulation. J Biol Chem. 2001;276(15):12128–34.
89. Huang R, Zhu WJ, Li J, Gu YQ. The changes of stage distribution of seminiferous epithelium cycle and its correlations with Leydig cell stereological parameters in aging men. Pathol Res Pract. 2014;210(12):991–6.
90. Samanta L, Swain N, Ayaz A, Venugopal V, Agarwal A. Post-Translational Modifications in

sperm Proteome: The Chemistry of Proteome diversifications in the Pathophysiology of male factor infertility. Biochim Biophys Acta. 2016;1860(7):1450–65.
91. de Las Rivas J, Fontanillo C. Protein-protein interactions essentials: Key concepts to building and analyzing interactome networks. PLoS Comput Biol. 2010;6(6):1–8.
92. Phizicky EM, Fields S. Protein-Protein Interactions: Methods for Detection and Analysis. Microbiol Rewiews. 1995;59(1):94–123.
93. Arkin MR, Tang Y, Wells JA. Small-molecule inhibitors of protein-protein interactions: Progressing toward the reality. Chem Biol. 2014;21(9):1102–14.
94. Zhang D, Wang J, Xu D. Cell-penetrating peptides as noninvasive transmembrane vectors for the development of novel multifunctional drug-delivery systems. J Control Release. 2016;229(81170255):130–9.
95. Higueruelo AP, Jubb H, Blundell TL. Protein-protein interactions as druggable targets: Recent technological advances. Curr Opin Pharmacol. 2013;13(5):791–6.
96. Howl J, Jones S. Insights into the molecular mechanisms of action of bioportides: a strategy to target protein-protein interactions. Expert Rev Mol Med. 2015;17:1–18.
97. Kristensen M, Birch D, Nielsen HM. Applications and challenges for use of cell-penetrating peptides as delivery vectors for peptide and protein cargos. Int J Mol Sci. 2016;17(2).
98. Svensen N, Walton JGA, Bradley M. Peptides for cell-selective drug delivery. Trends Pharmacol Sci. 2012;33(4):186–92.
99. Dinca A, Chien WM, Chin MT. Intracellular delivery of proteins with cell-penetrating peptides for therapeutic uses in human disease. Int J Mol Sci. 2016;17(2).
100. Kristensen M, Nielsen HM. Cell-Penetrating Peptides as Carriers for Oral Delivery of Biopharmaceuticals. Basic Clin Pharmacol Toxicol. 2016;118(2):99–106.
101. Zahid M, Robbins PD. Cell-type specific penetrating peptides: Therapeutic promises and challenges. Molecules. 2015;20(7):13055–70.
102. Howl J, Matou-Nasri S, West DC, Farquhar M, Slaninová J, Östenson CG, Zorko M, Östlund P, Kumar S, Langel Ü, McKeating J, Jones S. Bioportide: An emergent concept of bioactive cell-penetrating peptides. Cell Mol Life Sci. 2012;69(17):2951–66.
103. Li H, Tsui TY, Ma W. Intracellular delivery of molecular cargo using cell-penetrating peptides and the combination strategies. Int J Mol Sci. 2015;16(8):19518–36.
104. Green M, Ishino M, Loewenstein PM. Mutational analysis of HIV-1 Tat minimal domain peptides: Identification of trans-dominant mutants that suppress HIV-LTR-driven gene expression. Cell. 1989;58(1):215–23.
105. Derossi D, Joliot AH, Chassaing G, Prochiantz A. The third helix of the Antennapedia homeodomain translocates through biological membranes. J Biol Chem. 1994;269(14):10444–50.
106. Wender PA, Mitchell DJ, Pattabiraman K, Pelkey ET, Steinman L, Rothbard JB. The design, synthesis, and evaluation of molecules that enable or enhance cellular uptake: Peptoid molecular transporters. Proc Natl Acad Sci. 2000;97(24):13003–8.
107. Mai JC, Shen H, Watkins SC, Cheng T, Robbins PD. Efficiency of protein transduction is cell type-dependent and is enhanced by dextran sulfate. J Biol Chem. 2002;277(33):30208–18.
108. Mi Z, Mai J, Lu X, Robbins PD. Characterization of a Class of Cationic Peptides Able to Facilitate Efficient Protein Transduction in Vitro and in Vivo. Mol Ther. 2000;2(4):339–47.
109. Harreither E, Rydberg HA, Åmand HL, Jadhav V, Fliedl L, Benda C, Esteban MA, Pei D, Borth N, Grillari-Voglauer R, Hommerding O, Edenhofer F, Nordén B, Grillari J. Characterization of a novel cell penetrating peptide derived from human Oct4. Cell Regen. 2014;3(1):2.
110. Massaoka MH, Matsuo AL, Figueiredo CR, Girola N, Faria CF, Azevedo RA, Travassos LR. A novel cell-penetrating peptide derived from WT1 enhances p53 activity, induces cell senescence and displays antimelanoma activity in xeno- and syngeneic systems. FEBS Open Bio. 2014;4(1):153–61.
111. de Coupade C, Fittipaldi A, Chagnas V, Michel M, Carlier S, Tasciotti E, Darmon A, Ravel D, Kearsey J, Giacca M, Cailler F. Novel human-derived cell-penetrating peptides for specific subcellular delivery of therapeutic biomolecules. Biochem J. 2005;390(2):407–18.
112. El-Andaloussi S, Johansson HJ, Holm T, Langel Ü. A Novel Cell-penetrating Peptide, M918, for Efficient Delivery of Proteins and Peptide Nucleic Acids. Mol Ther. 2007;15(10):1820–6.
113. Pooga M, Hällbrink M, Zorko M, Langel Ü. Cell penetration by transportan. FASEB J.

1998;12(1):67–77.
114. Oehlke J, Scheller A, Wiesner B, Krause E, Beyermann M, Klauschenz E, Melzig M, Bienert M. Cellular uptake of an alpha-helical amphipathic model peptide with the potential to deliver polar compounds into the cell interior non-endocytically. Biochim Biophys Acta - Biomembr. 1998;1414(1–2):127–39.
115. Jones S, Farquhar M, Martin A, Howl J. Intracellular translocation of the decapeptide carboxyl terminal of G i3α induces the dual phosphorylation of p42/p44 MAP kinases. Biochim Biophys Acta - Mol Cell Res. 2005;1745(2):207–14.
116. Morris MC, Depollier J, Mery J, Heitz F, Divita G. A peptide carrier for the delivery of biologically active proteins into mammalian cells. Nat Biotechnol. 2001;19(12):1173–6.
117. Kim W, Kim DW, Yoo DY, Chung JY, Hwang IK, Won MH, Choi SY, Jeon SW, Jeong JH, Hwang HS, Moon SM. Neuroprotective effects of PEP-1-Cu,Zn-SOD against ischemic neuronal damage in the rabbit spinal cord. Neurochem Res. 2012;37(2):307–13.
118. Nigatu AS, Vupputuri S, Flynn N, Neely BJ, Ramsey JD. Evaluation of cell-penetrating peptide/adenovirus particles for transduction of CAR-negative cells. J Pharm Sci. 2013;102(6):1981–93.
119. Wei Y, Li C, Zhang L, Xu X. Design of novel cell penetrating peptides for the delivery of trehalose into mammalian cells. Biochim Biophys Acta - Biomembr. 2014;1838(7):1911–20.
120. Lim J, Kim J, Duong T, Lee G, Kim J, Yoon J, Kim J, Kim H, Ruley HE, El-Rifai W, Jo D. Antitumor activity of cell-permeable p18(INK4c) with enhanced membrane and tissue penetration. Mol Ther. 2012;20(8):1540–9.
121. Lim J, Duong T, Do N, Do P, Kim J, Kim H, El-Rifai W, Earl Ruley H, Jo D. Antitumor activity of cell-permeable RUNX3 protein in gastric cancer cells. Clin Cancer Res. 2013;19(3):680–90.
122. Findlay DM, Houssami S, Lin HY, Myers DE, Brady CL, Darcy PK, Ikeda K, Martin TJ, Sexton PM. Truncation of the porcine calcitonin receptor cytoplasmic tail inhibits internalization and signal transduction but increases receptor affinity. Mol Endocrinol. 1994;8(12):1691–700.
123. Elmquist A, Hansen M, Langel U. Structure-activity relationship study of the cell-penetrating peptide pVEC. Biochim Biophys Acta. 2006;1758(6):721–9.
124. Elliott G, O'Hare P. Intercellular trafficking and protein delivery by a herpesvirus structural protein. Cell. 1997;88(2):223–33.
125. Dilber MS, Phelan A, Aints A, Mohamed AJ, Elliott G, Smith CI, O'Hare P. Intercellular delivery of thymidine kinase prodrug activating enzyme by the herpes simplex virus protein, VP22. Gene Ther. 1999;6(1):12–21.
126. Rhee M, Davis P. Mechanism of uptake of C105Y, a novel cell-penetrating peptide. J Biol Chem. 2006;281(2):1233–40.
127. Watkins CL, Brennan P, Fegan C, Takayama K, Nakase I, Futaki S, Jones AT. Cellular uptake, distribution and cytotoxicity of the hydrophobic cell penetrating peptide sequence PFVYLI linked to the proapoptotic domain peptide PAD. J Control Release. 2009;140(3):237–44.
128. Cai D, Gao W, He B, Dai W, Zhang H, Wang X, Wang J, Zhang X, Zhang Q. Hydrophobic penetrating peptide PFVYLI-modified stealth liposomes for doxorubicin delivery in breast cancer therapy. Biomaterials. 2014;35(7):2283–94.
129. Gottschalk S, Sparrow JT, Hauer J, Mims MP, Leland FE, Woo SLC, Smith LC. A novel DNA-peptide complex for efficient gene transfer and expression in mammalian cells. Gene Ther. 1996;3(5):448–57.
130. Scheller A, Oehlke J, Wiesner B, Dathe M, Krause E, Beyermann M, Melzig M, Bienert M. Structural requirements for cellular uptake of alpha-helical amphipathic peptides. J Pept Sci. 1999;5(4):185–94.
131. Jones S, Martel C, Belzacq-Casagrande AS, Brenner C, Howl J. Mitoparan and target-selective chimeric analogues: Membrane translocation and intracellular redistribution induces mitochondrial apoptosis. Biochim Biophys Acta - Mol Cell Res. 2008;1783(5):849–63.
132. Zahid M, Phillips BE, Albers SM, Giannoukakis N, Watkins SC, Robbins PD. Identification of a cardiac specific protein transduction domain by in Vivo biopanning using a M13 phage peptide display library in mice. PLoS One. 2010;5(8).
133. McConnell SJ, Thon VJ, Spinella DG. Isolation of fibroblast growth factor receptor binding

sequences using evolved phage display libraries. Comb Chem High Throughput Screen. 1999;2(3):155–63.
134. Mi Z, Lu X, Mai JC, Ng BG, Wang G, Lechman ER, Watkins SC, Rabinowich H, Robbins PD. Identification of a synovial fibroblast-specific protein transduction domain for delivery of apoptotic agents to hyperplastic synovium. Mol Ther. 2003;8(2):295–305.
135. Zong X, Jiang D, Li G, Cai J. Construction of keratinocyte growth factor phage active peptides for the promotion of epidermal cell proliferation. Zhonghua Yi Xue Za Zhi. 2013;93(14):1058–62.
136. Jones S, Holm T, Mäger I, Langel Ü, Howl J. Characterization of Bioactive Cell Penetrating Peptides from Human Cytochrome c: Protein Mimicry and the Development of a Novel Apoptogenic Agent. Chem Biol. 2010;17(7):735–44.
137. Durzyńska J, Przysiecka Ł, Nawrot R, Barylski J, Nowicki G, Warowicka A, Musidlak O, Goździcka-Józefiak A. Viral and other cell-penetrating peptides as vectors of therapeutic agents in medicine. J Pharmacol Exp Ther. 2015;354(1):32–42.
138. Jones S, Lukanowska M, Suhorutsenko J, Oxenham S, Barratt C, Publicover S, Copolovici DM, Langel Ü, Howl J. Intracellular translocation and differential accumulation of cell-penetrating peptides in bovine spermatozoa: evaluation of efficient delivery vectors that do not compromise human sperm motility. Hum Reprod. 2013;28(7):1874–89.
139. Jones S, Uusna J, Langel Ü, Howl J. Intracellular Target-Specific Accretion of Cell Penetrating Peptides and Bioportides: Ultrastructural and Biological Correlates. Bioconjug Chem. 2016;27(1):121–9.
140. Nya-Ngatchou J-J, Amory JK. New approaches to male non-hormonal contraception. Contraception. 2013;87(3):296–9.
141. Finer LB, Henshaw SK. Abortion Incidence and Services In the United States in 2000. Perspect Sex Reprod Health. 2003;35(1):6–15.
142. Jones RK, Darroch JE, Henshaw SK. Contraceptive use among U.S. women having abortions in 2000-2001. Perspect Sex Reprod Health. 2002;34(6):294–303.
143. Singh S, Sedgh G, Hussain R. Unintended Pregnancy: Worldwide Levels, Trends, and Outcomes. Stud Fam Plann. 2010;41(4):241–50.
144. Kogan P, Wald M. Male contraception: History and development. Urol Clin North Am. 2014;41(1):145–61.
145. Chao J, Page ST, Anderson RA. Male contraception. Best Pract Res Clin Obstet Gynaecol. 2014;28(6):845–57.
146. World Health Organization. Examination and processing of human semen. Fifth. 2010. 286 p.
147. Ahmad M, Ahmad N, Riaz A, Anzar M. Sperm survival kinetics in different types of bull semen: Progressive motility, plasma membrane integrity, acrosomal status and reactive oxygen species generation. Reprod Fertil Dev. 2015;27(5):784–93.
148. Silva JV, Yoon S, De Bock PJ, Goltsev A V., Gevaert K, Mendes JFF, Fardilha M. Construction and analysis of a human testis/sperm-enriched interaction network: Unraveling the PPP1CC2 interactome. Biochim Biophys Acta - Gen Subj. 2017;1861(2):375–85.
149. Gupta N, Bandeira N, Keich U, Pevzner PA. Target-decoy approach and false discovery rate: When things may go wrong. J Am Soc Mass Spectrom. 2011;22(7):1111–20.
150. Elias JE, Gygi SP. Target-Decoy Search Strategy for Mass Spectrometry-Based Proteomics. In: Methods in molecular biology (Clifton, NJ). NIH Public Access; 2010. p. 55–71.
151. Keilhauer EC, Hein MY, Mann M. Accurate Protein Complex Retrieval by Affinity Enrichment Mass Spectrometry (AE-MS) Rather than Affinity Purification Mass Spectrometry (AP-MS). Mol Cell Proteomics. 2015;14(1):120–35.
152. Li J, Liu F, Liu X, Liu J, Zhu P, Wan F, Jin S, Wang W, Li N, Liu J, Wang H. Mapping of the human testicular proteome and its relationship with that of the epididymis and spermatozoa. Mol Cell Proteomics. 2011;10(3):M110.004630.
153. Hamada A, Sharma R, Du Plessis SS, Willard B, Yadav SP, Sabanegh E, Agarwal A. Two-dimensional differential in-gel electrophoresis-based proteomics of male gametes in relation to oxidative stress. Fertil Steril. 2013;99(5):1216–1226.e2.
154. Paasch U, Heidenreich F, Pursche T, Kuhlisch E, Kettner K, Grunewald S, Kratzsch J, Dittmar G, Glander H-J, Hoflack B, Kriegel TM. Identification of increased amounts of eppin protein complex components in sperm cells of diabetic and obese individuals by difference

gel electrophoresis. Mol Cell Proteomics [Internet]. 2011 Aug [cited 2017 May 10];10(8):M110.007187. Available from: http://www.ncbi.nlm.nih.gov/pubmed/21525168
155. Intasqui P, Camargo M, Del Giudice PT, Spaine DM, Carvalho VM, Cardozo KHM, Cedenho AP, Bertolla RP. Unraveling the sperm proteome and post-genomic pathways associated with sperm nuclear DNA fragmentation. J Assist Reprod Genet. 2013;30(9):1187–202.
156. McReynolds S, Dzieciatkowska M, Stevens J, Hansen KC, Schoolcraft WB, Katz-Jaffe MG. Toward the identification of a subset of unexplained infertility: A sperm proteomic approach. Fertil Steril. 2014;102(3):692–9.
157. Amaral A, Paiva C, Attardo Parrinello C, Estanyol JM, Ballescà JL, Ramalho-Santos J, Oliva R. Identification of proteins involved in human sperm motility using high-throughput differential proteomics. J Proteome Res. 2014;13(12):5670–84.
158. Kriegel TM, Heidenreich F, Kettner K, Pursche T, Hoflack B, Grunewald S, Poenicke K, Glander HJ, Paasch U. Identification of diabetes- and obesity-associated proteomic changes in human spermatozoa by difference gel electrophoresis. Reprod Biomed Online. 2009;19(5):660–70.
159. Légaré C, Droit A, Fournier F, Bourassa S, Force A, Cloutier F, Tremblay R, Sullivan R. Investigation of male infertility using quantitative comparative proteomics. J Proteome Res. 2014;13(12):5403–14.
160. Xu W, Hu H, Wang Z, Chen X, Yang F, Zhu Z, Fang P, Dai J, Wang L, Shi H, Li Z, Qiao Z. Proteomic characteristics of spermatozoa in normozoospermic patients with infertility. J Proteomics. 2012;75(17):5426–36.
161. Shen S, Wang J, Liang J, He D. Comparative proteomic study between human normal motility sperm and idiopathic asthenozoospermia. World J Urol. 2013;31(6):1395–401.
162. Liu FJ, Liu X, Han JL, Wang YW, Jin SH, Liu XX, Liu J, Wang WT, Wang WJ. Aged men share the sperm protein PATE1 defect with young asthenozoospermia patients. Hum Reprod. 2014;30(4):861–9.
163. Liao T-T, Xiang Z, Zhu W-B, Fan L-Q. Proteome analysis of round-headed and normal spermatozoa by 2-D fluorescence difference gel electrophoresis and mass spectrometry. Asian J Androl. 2009;11(6):683–93.
164. Silva JV. Proteínas do espermatozoide como alvos para contraceção e biomarcadores de fertilidade. Universidade de Aveiro; 2016.
165. Buranaamnuay K, Seesuwan K, Saikhun K. Preliminary study on effects of bovine frozen semen storage using a liquid nitrogen-independent method on the quality of post-thaw spermatozoa. Anim Reprod Sci. 2016;172:32–8.
166. Ursini F, Maiorino M, Valente M, Ferri L, Gregolin C. Purification from pig liver of a protein which protects liposomes and biomembranes from peroxidative degradation and exhibits glutathione peroxidase activity on phosphatidylcholine hydroperoxides. Biochim Biophys Acta (BBA)/Lipids Lipid Metab. 1982;710(2):197–211.
167. Ursini F, Heim S, Kiess M, Maiorino M, Roveri A, Wissing J, Flohé L. Dual function of the selenoprotein PHGPx during sperm maturation. Science (80-). 1999;285(5432):1393–6.
168. Ingold I, Aichler M, Yefremova E, Roveri A, Buday K, Doll S, Tasdemir A, Hoffard N, Wurst W, Walch A, Ursini F, Angeli JPF, Conrad M. Expression of a catalytically inactive mutant form of glutathione peroxidase 4 (Gpx4) confers a dominant-negative effect in male fertility. J Biol Chem. 2015;290(23):14668–78.
169. Brigelius-Flohé R. Tissue-specific functions of individual glutathione peroxidases. In: Free Radical Biology and Medicine. 1999. p. 951–65.
170. Imai H, Hakkaku N, Iwamoto R, Suzuki J, Suzuki T, Tajima Y, Konishi K, Minami S, Ichinose S, Ishizaka K, Shioda S, Arata S, Nishimuřa M, Naito S, Nakagawa Y. Depletion of selenoprotein GPx4 in spermatocytes causes male infertility in mice. J Biol Chem. 2009;284(47):32522–32.
171. Schneider M, Forster H, Boersma A, Seiler A, Wehnes H, Sinowatz F, Neumuller C, Deutsch MJ, Walch A, Hrabe de Angelis M, Wurst W, Ursini F, Roveri A, Maleszewski M, Maiorino M, Conrad M. Mitochondrial glutathione peroxidase 4 disruption causes male infertility. FASEB J. 2009;23(9):3233–42.

Supplementary Data

Supplementary Table 1 - Solutions used in the experiments.

Quantitative uptake analysis		
1% Trypsin (wt/vol)	For 10 ml of deionized water dissolve 0,1g of trypsin. Adjust pH to 7.5-8.5 with NaOH.	
0,1 M NaOH	For 100 ml of deionized water dissolve 0,4g of NaOH.	
Co-immunoprecipitation		
1X RIPA + 0,1mM PMSF (lysis buffer)	For a final volume of 1 ml add 100µl of 10X RIPA and 1µl of PMSF 0,1M to 1799µl of deionized water.	
Trypsin digestion buffer	For a final volume of 50 ml add 1 mL of 1M Tris-HCl pH 8.0 and 0,1 mL of 1M $CaCl_2$ to 50 ml of deionized water.	
$CaCl_2$ 1M	For a final volume of 50 ml dissolve 7,35g CaCl2 dihydrated in 50 ml of deionized water.	
Western Blot		
Running gel 10% (2 gels, 1,5 mm thickness)	ddH2O Tris 1.5M pH8.8 Acrylamide 40% Bisacrylamide 2% SDS 10% APS 10% TEMED	7,720 ml 5,000 ml 4,920 ml 1,960 ml 0,200 ml 0,100 ml 0,020 ml
Running gel 15% (2 gels, 1,5 mm thickness)	ddH2O Tris 1.5M pH8.8 Acrylamide 40% Bisacrylamide 2% SDS 10% APS 10% TEMED	4,2800 ml 5,000 ml 7,360 ml 2,960 ml 0,200 ml 0,100 ml 0,020 ml
Stacking gel 4% (2 gels, 1,5 mm thickness)	ddH2O Tris 0,5M pH6.8 Acrylamide 40% Bisacrylamide 2% SDS 10% APS 10% TEMED	4,736 ml 2,000 ml 0,784 ml 0,320 ml 0,080 ml 0,040 ml 0,008 ml
Tris-HCl 1.5M pH 8.8 buffer	For 1L dissolve 181,5g Tris in 800 mL deionized water. Adjust pH at 8.8 with HCl and make up to 1L with deionized water.	
Tris-HCl 0,5M pH 6.8 buffer	For 1L dissolve 60g Tris in 800 mL deionized water. Adjust pH at 6.8 with HCl and make up to 1L with deionized water.	
10% APS (ammonium persulfate)	For 10 ml of deionized water add 1g of APS.	
10% SDS (sodium dodecilsulfate)	For 500 mL of deionized water dissolve 50g of SDS.	
4X Loading gel buffer	For 10 ml add 44 ml glycerol, 250 µl Tris-HCl 0.5M pH	

	6.8 buffer, 0,8g SDS, 0,2 ml β-mercaptoethanol and 3,3 ml deionized water. Add bromophenol blue (a small amount). Keep it at RT for short periods or at 4ºC for longer periods.
Tris-Gly 10X Stock	For 1L dissolve 30,30g Tris (250mM) and 144,10g Gly (1,92 M) in 1L of deionized water.
Running buffer 1X	For 1L add 800 ml deionized water, 100 ml Tris-Gly 10X and 10 ml 10%SDS. Make up to 1L with deionized water.
Transfer buffer 1X	For 1L add 100 ml Tris-Gly 10X to 700 ml of deionized water and 200 ml methanol.
10X TBS Stock (Tris buffered saline)	For 0,5 L dissolve 6,055g Tris in deionized water and adjust pH at 8.0. Add 43,8325 g NaCl and make up to 500 ml with deionized water.
1X TBST (TBS + Tween 20)	For 1 L add 100 ml TBS 10X and 500 µl Tween-20 to 900 ml of deionized water.
5% BSA in TBST 1X	For 100 ml of solution dissolve 5 g of BSA in TBST 1X.
Ponceau S.	For 100 ml of Ponceau S. staining solution dissolve 0,1 g of Ponceau S. in 5 ml of acid acetic and fill up to 100 ml with deionized water.

Supplementary Table 2 - Basic semen parameters of 6 random men providing semen samples for routine analysis. PM, progressive motility; NPM, non-progressive motility; IM, immotile spermatozoa; MP, midpiece; ERC, excess of residual cytoplasm.

Volunteer	Volume (ml)	Concentration (x 10^6/ml)	No. spermatozoa (x 10^6)	Motility (%)				Morphology (%)				
				Total	PM	NPM	I	Normal	Head	MP	Tail	ERC
1	2.4	84	201.6	55	44	11	45	10	88	48	42	1
2	1.9	31	58.9	65	51	14	35	14	68	36	36	0
3	2.8	71	198.8	61	41	20	39	5	87	55	46	0
4	1.6	180	288	63	54	9	37	16	80	59	42	0
5	3.8	68	258.4	55	46	9	45	6	70	58	44	0
6	1.2	38	45.6	49	32	17	51	21	68	38	29	0

Supplementary Table 3 - Standards for BCA assay

Standards	BSA (µl)	1% SDS (µl)	Protein (µg)
P_0	-	25	0
P_1	0.5	24.5	1
P_2	1	24	2
P_3	2.5	22.5	5
P_4	5	20	10
P_5	10	15	20

Supplementary Table 4 - Temporal-dependent quantitative analysis of peptide translocation into bovine spermatozoa. Bovine spermatozoa were incubated with 5 μM TAMRA-labeled bioactive CPP for 15, 30 and 60 min at 37ºC. Data are expressed as fluorescence. Three independent experiments were performed in triplicate.

		Experiment 1			Experiment 2			Experiment 3		
Condition		1	2	3	1	2	3	1	2	3
0 min	NC				4473	3039	2695	1641	87	229
	AKAP4-BM				24209	14724	19681	7598	6230	9061
	AKAP4-BM M				5163	5566	4852	1172	4762	1462
	PPP1CC2-CT				13331	11564	15691	3247	4165	2903
15 min	NC	181	156	167	114	101	125	40	51	57
	AKAP4-BM	20025	33081	33527	17050	14700	13737	6256	5380	6424
	AKAP4-BM M	6171	3637	4391	6471	4189	7037	4936	1902	2174
	PPP1CC2-CT	13432	14383	11398	13559	14787	18710	6921	7038	7465
30 min	NC	200	162	165	321	1406	1085	2034	1901	340
	AKAP4-BM	30473	20887	17951	19003	20275	24131	11892	12604	37253
	AKAP4-BM M	3630	3413	3599	6899	11953	6057	2946	2392	2077
	PPP1CC2-CT	8651	7973	8234	6523	9440	13418	7357	4463	3373
60 min	NC	189	205	166	1866	976	1032	2847	237	239
	AKAP4-BM	36461	33310	33785	39592	25402	37957	15764	12404	16529
	AKAP4-BM M	3817	3754	3445	14289	8803	10693	4099	6299	3843
	PPP1CC2-CT	9772	10919	8365	25027	26192	24467	7899	7853	10144

Supplementary Table 5 – Concentration-dependent quantitative analysis of peptide translocation into bovine spermatozoa. Bovine spermatozoa were incubated with 5 μM, 7,5 μM and 10 μM TAMRA-labeled bioactive CPP for min at 37ºC. Data are expressed as fluorescence. Three independent experiments were performed in triplicate.

		Experiment 1			Experiment 2			Experiment 3		
Condition		1	2	3	1	2	3	1	2	3
AKAP4	0	228	259	262	114	101	125	40	51	57
	5	25457	17710	22705	17050	14700	13737	6256	5380	6424
	7,5	16823	44164	38758	21278	21033	19793	8613	10991	9520
	10	40506	37796	37053	25475	31087	27379	17791	13948	13422
AKAP4-BM M	0	228	259	262	114	101	125	40	51	57
	5	3254	2681	2677	6471	4189	7037	4936	1902	2174
	7,5	4756	5164	6224	5628	10703	13309	2252	3557	3324
	10	4051	5365	3803	11122	10930	8894	3313	3756	4155
PPP1CC2-CT	0	228	259	262	114	101	125	40	51	57
	5	7575	6379	5289	13559	14787	18710	6921	7038	7465
	7,5	12655	13818	16268	8787	17967	11532	9213	9279	11705
	10	17259	15094	12270	24928	15877	22330	10502	8224	9806

Supplementary Table 6 – Descriptive analysis; Statistical measures: Mean and standard deviation (SD) associated with CPP treatments in bovine spermatozoa; NC, negative control; PM, progressive motility; NPM, non-progressive motility; IM, immotile spermatozoa. Data are expressed as mean of three independent experiments performed in triplicate.

		15 min							
		PPP1CC2-CT		AKAP4-BM		AKAP4-BM M		NC	
		5 µM	10 µM	5 µM	10 µM	5 µM	10 µM	5 µM	10 µM
PM fast (%)	Mean	14,5	15,0	10,0	7,7	21,5	29,6	29,5	29,5
	SD	6,9	7,8	4,3	5,7	7,1	15,8	7,8	7,8
PM slow (%)	Mean	5,9	8,3	7,1	8,8	8,8	10,3	9,9	9,9
	SD	2,2	4,3	2,6	3,7	3,7	4,2	4,4	4,4
NPM (%)	Mean	21,4	26,2	26,8	24,4	25,5	21,0	23,3	23,3
	SD	2,6	6,2	6,5	7,5	5,5	5,7	2,7	2,7
IM (%)	Mean	58,1	50,5	56,1	62,0	44,2	39,1	37,3	37,3
	SD	9,3	13,3	8,3	13,1	12,3	16,1	9,6	9,6

Supplementary Table 7 – Inferential statistics; Test for differences between means of two independent groups associated with PPP1CC2-CT peptide treatments in bovine spermatozoa. NC, negative control; PM, progressive motility; NPM, non-progressive motility; IM, immotile spermatozoa. Data are expressed as mean of three independent experiments performed in triplicate.

Variable	Groups (5uM)	Test	Sig. (2 tailed)	Interpretation Unilateral Test
				% of spermatozoa (variable) is significantly higher in
PM fast	PPP1CC2-CT / NC	Student's T-test	0,001	NC
PM slow		Student's T-test	0,026	NC
NPM		Student's T-test	0,154	-
IM		Student's T-test	0	PPP1CC2-CT
Variable	**Groups (10uM)**	**Test**	**Sig. (2-tailed)**	**Interpretation Unilateral Test**
				% of spermatozoa (variable) is significantly higher in
PM fast	PPP1CC2-CT / NC	Student's T-test	0,001	NC
PM slow		Student's T-test	0,423	-
NPM		Student's T-test	0,234	-
IM		Student's T-test	0,029	PPP1CC2-CT

Supplementary Table 8 - Inferential statistics; Test for differences between means of two independent groups associated with AKAP4 peptides treatments in bovine spermatozoa. NC, negative control; PM, progressive motility; NPM, non-progressive motility; IM, immotile spermatozoa. Data are expressed as mean of three independent experiments performed in triplicate.

Variable	**Groups (5uM)**	**Test**	**Sig. (2 tailed)**	**Interpretation Unilateral Test**
				% of spermatozoa (variable) is significantly higher in
PM fast	AKAP4 BM / NC	Student's T-test	0	NC
PM slow		Student's T-test	0,114	-
NPM		Student's T-test	0,171	-
IM		Student's T-test	0	AKAP4-BM
Variable	**Groups (10uM)**	**Test**	**Sig. (2 tailed)**	**Interpretation Unilateral Test**
				% of spermatozoa (variable) is significantly higher in
PM fast	AKAP4 BM / NC	Student's T-test	0	NC
PM slow		Student's T-test	0,042	NC
NPM		Student's T-test	0,69	-
IM		Student's T-test	0	AKAP4-BM
Variable	**Groups (5uM)**	**Test**	**Sig. (2 tailed)**	**Interpretation Unilateral Test**
				% of spermatozoa (variable) is significantly higher in
PM fast	AKAP4 BM M / NC	Student's T-test	0,039	NC
PM slow		Student's T-test	0,564	-
NPM		Student's T-test	0,308	-
IM		Student's T-test	0,204	-
Variable	**Groups (10uM)**	**Test**	**Sig. (2 tailed)**	**Interpretation Unilateral Test**
				% of spermatozoa (variable) is significantly higher in
PM fast	AKAP4 BM M / NC	Student's T-test	0,981	-
PM slow		Student's T-test	0,862	-
NPM		Student's T-test	0,283	-
IM		Student's T-test	0,773	-
Variable	**Groups (5uM)**	**Test**	**Sig. (2 tailed)**	**Interpretation Unilateral Test**
				% of spermatozoa (variable) is significantly higher in
PM fast	AKAP4 BM / AKAP4 BM M	Student's T-test	0,001	AKAP4-BM M
PM slow		Student's T-test	0,271	-
NPM		Student's T-test	0,657	-
IM		Student's T-test	0,028	AKAP4-BM
Variable	**Groups (10uM)**	**Test**	**Sig. (2 tailed)**	**Interpretation Unilateral Test**
				% of spermatozoa (variable) is significantly higher in
PM fast	AKAP4 BM / AKAP4 BM M	Student's T-test	0,003	AKAP4-BM M
PM slow		Student's T-test	0,025	AKAP4-BM M
NPM		Student's T-test	0,289	-
IM		Student's T-test	0,004	AKAP4-BM

Supplementary Table 9 - PPP1CC2-CT peptide's putative interactors identified by LC-MS/MS analysis.

Uniprot ID	Protein name	Gene name	Peptides	Razor + unique peptides	Unique peptides	Sequence coverage [%]	Unique + razor sequence coverage [%]	Unique sequence coverage [%]	Score
Q00577	Transcriptional activator protein Pur-alpha	PURA	10	10	10	39,8	39,8	39,8	323,31
P02788	Lactotransferrin	LTF	20	20	20	30,7	30,7	30,7	323,31
Q9Y2T7	Y-box-binding protein 2	YBX2	5	2	2	19	9,1	9,1	171,2
Q75WM6	Testis-specific H1 histone	H1FNT	3	3	3	12,2	12,2	12,2	24,443
P11940	Polyadenylate-binding protein 1	PABPC1	17	17	12	26,6	26,6	18,2	323,31
P43155	Carnitine O-acetyltransferase	CRAT	14	14	14	25,4	25,4	25,4	109,49
P37108	Signal recognition particle 14 kDa protein	SRP14	5	5	5	33,1	33,1	33,1	84,675
Q6NUI6	Chondroadherin-like protein	CHADL	6	6	6	12,6	12,6	12,6	31,79
O75569	Interferon-inducible double-stranded RNA-dependent protein kinase activator A	PRKRA	6	6	6	24,9	24,9	24,9	51,187
P48729 Q8N752	Casein kinase I isoform alpha Casein kinase I isoform alpha-like	CSNK1A1 CSNK1A1L	6	6	6	19,3	19,3	19,3	12,46
Q7L2E3	Putative ATP-dependent RNA helicase DHX30	DHX30	14	14	14	16,2	16,2	16,2	42,423
Q9Y4P3	Transducin beta-like protein 2	TBL2	6	6	6	17,2	17,2	17,2	30,489
P04279	Semenogelin-1	SEMG1	15	15	12	39,4	39,4	32	203,77
Q8N0Z8	tRNA pseudouridine synthase-like 1	PUSL1	6	6	6	26,1	26,1	26,1	21,378
A4D1T9	Probable inactive serine protease 37	PRSS37	4	4	4	18,3	18,3	18,3	41,194
Q96A08	Histone H2B type 1-A	HIST1H2BA	6	3	3	40,9	19,7	19,7	248,39
Q9BTE6	Alanyl-tRNA editing protein Aarsd1	AARSD1	7	7	7	26,2	26,2	26,2	48,729
Q9Y2C4	Nuclease EXOG, mitochondrial	EXOG	4	4	4	16,3	16,3	16,3	9,8266
O95782 O94973	AP-2 complex subunit alpha-1 AP-2 complex subunit alpha-2	AP2A1 AP2A2	4	4	4	5	5	5	6,8889
Q07021	Complement component 1 Q subcomponent-binding protein, mitochondrial	C1QBP	3	3	3	15,6	15,6	15,6	6,2494
Q6X784	Zona pellucida-binding protein 2	ZPBP2	4	4	4	13,6	13,6	13,6	15,524
Q14997	Proteasome activator complex subunit 4	PSME4	12	12	12	9,2	9,2	9,2	43,811

Uniprot ID	Protein name	Gene name	Peptides	Razor + unique peptides	Unique peptides	Sequence coverage [%]	Unique + razor sequence coverage [%]	Unique sequence coverage [%]	Score
P61626	Lysozyme C	LYZ	2	2	2	14,2	14,2	14,2	11,965
Q9UHI8	A disintegrin and metalloproteinase with thrombospondin motifs 1	ADAMTS1	2	2	2	3	3	3	3,3085
Q9H0B8	Cysteine-rich secretory protein LCCL domain-containing 2	CRISPLD2	5	5	5	13,3	13,3	13,3	13,505
Q02383	Semenogelin-2	SEMG2	9	6	6	22,7	16,8	16,8	25,709
P10323	Acrosin	ACR	8	8	8	17,1	17,1	17,1	119,51
Q8TDZ2	Protein-methionine sulfoxide oxidase MICAL1	MICAL1	6	6	6	8,4	8,4	8,4	12,087
Q92820	Gamma-glutamyl hydrolase	GGH	7	7	7	25,2	25,2	25,2	21,552
P61163	Alpha-centractin	ACTR1A	10	10	8	35,6	35,6	31,1	156,13
P05154	Plasma serine protease inhibitor	SERPINA5	3	3	3	9,6	9,6	9,6	4,5206
Q8IVS2	Malonyl-CoA-acyl carrier protein transacylase, mitochondrial	MCAT	3	3	3	13,8	13,8	13,8	10,428
Q13618	Cullin-3	CUL3	19	19	19	29,6	29,6	29,6	192,32
P36969	Phospholipid hydroperoxide glutathione peroxidase, mitochondrial	GPX4	2	2	2	13,2	13,2	13,2	7,9002
Q16698	2,4-dienoyl-CoA reductase, mitochondrial	DECR1	13	13	13	50,1	50,1	50,1	323,31
Q13011	Delta(3,5)-Delta(2,4)-dienoyl-CoA isomerase, mitochondrial	ECH1	2	2	2	7,3	7,3	7,3	4,224
P10909	Clusterin	CLU	8	8	8	22,3	22,3	22,3	142,13
O75390	Citrate synthase, mitochondrial	CS	10	10	10	29,2	29,2	29,2	67,451
P36957	Dihydrolipoyllysine-residue succinyltransferase component of 2-oxoglutarate dehydrogenase complex, mitochondrial	DLST	2	2	2	4,6	4,6	4,6	5,4474
P67809 P16989	Nuclease-sensitive element-binding protein 1 Y-box-binding protein 3	YBX1 YBX3	6	6	3	26,5	26,5	15,4	323,31
P36873	Serine/threonine-protein phosphatase PP1-gamma catalytic subunit	PPP1CC	4	4	4	11,1	11,1	11,1	26,987
Q9Y285	Phenylalanine--tRNA ligase alpha subunit	FARSA	4	4	4	9,8	9,8	9,8	19,284
Q9UGP8	Translocation protein SEC63 homolog	SEC63	2	2	2	2,6	2,6	2,6	2,5174
Q9UQ80	Proliferation-associated protein 2G4	PA2G4	7	7	7	17	17	17	32,19
Q6JEL2	Kelch-like protein 10	KLHL10	3	3	3	5,9	5,9	5,9	3,9091
Q92523	Carnitine O-palmitoyltransferase 1, muscle isoform	CPT1B	7	7	7	10,6	10,6	10,6	18,443
Q04837	Single-stranded DNA-binding protein, mitochondrial	SSBP1	4	4	4	33,8	33,8	33,8	43,69

Supplementary Figure 1 – Ponceau S. staining used as loading control in blot overlay.

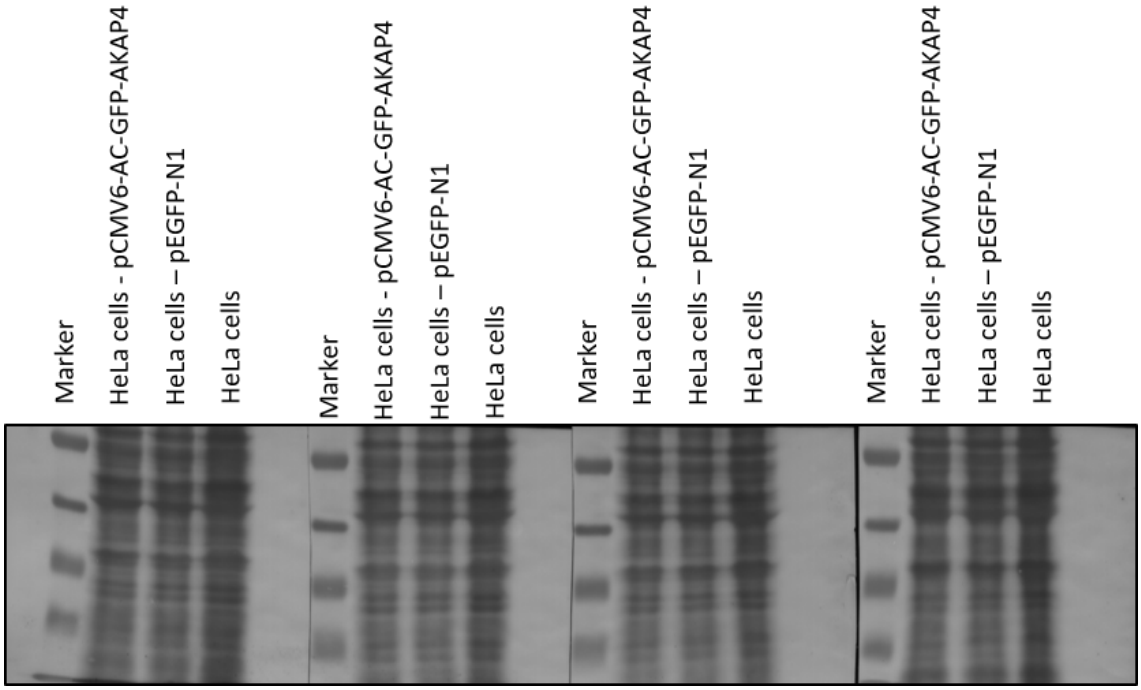

Supplementary Figure 2 – Immunoblot with mouse anti-β-tubulin antibody used as loading control in blot overlay.

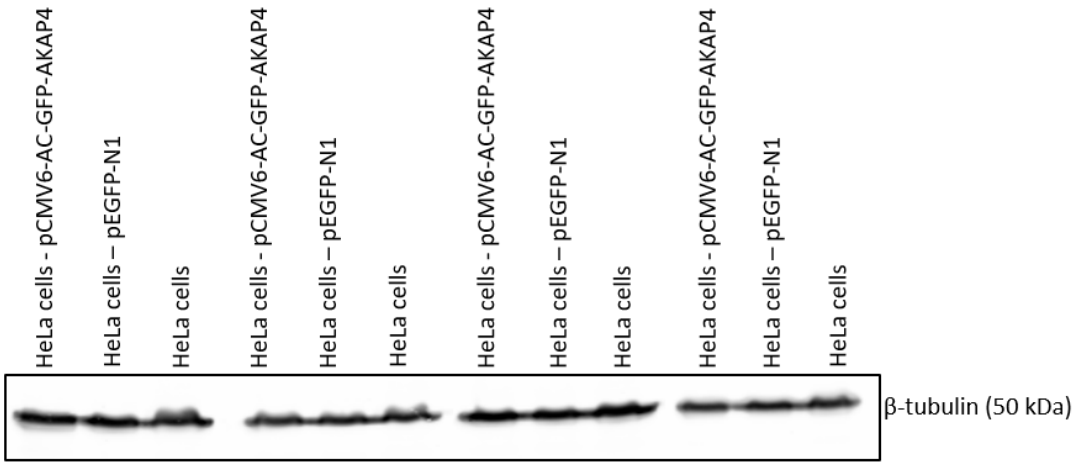

IB: Mouse anti-β-tubulina